LA-SUB--96-1

Final Project Report

on

HYDROLOGIC REVIEW SERVICES

under

Subcontract 9 - XG3 - 6600H - 1

for period

May 24, 1993, to December 31, 1993

to

University of California
Los Alamos National Laboratory
Attn: R.N. Tokay
P.O. Box 990, MS P274
Los Alamos, NM 87545

from

John A. Hoopes, Professor
and Project Director
1261B Engineering Hall
Civil & Environmental Engineering Department
University of Wisconsin
1415 Engineering Drive
Madison, WI 53706

H Hill

October 1995

DISCLAIMER

ABSTRACT

The goal of this project was to conduct field and laboratory investigations with model simulations of the transport and distribution by water and sediment movement of depleted uranium and heavy metals from weapons testing activities in TA 39 (Big Buck Canyon) at Los Alamos National Laboratory (LANL). This work built on the earlier and continuing studies in Potrillo Canyon at LANL and sought to develop and test methods which can be applied to contaminant movement in other canyon watersheds at LANL. This work, initiated in May 1993, is continuing. This report summarizes the accomplishments from May 1993 through May 1994.

BACKGROUND

There is need for technically defensible field and laboratory investigations and appropriate hydrologic transport models for the unique hydrologic and materials transport scenarios in watersheds at LANL.

OBJECTIVES

1.0 Provide hydrologic support and review services for hydrologic and hydrogeologic documents

2.0 Conduct investigations and literature review on uranium partitioning

- 2.1 Extend investigations and literature review to other elements
- 2.2 Conduct laboratory experiments on partitioning for various elements

3.0 Conduct hydraulic and hydrologic investigations using models of

- 3.1 Flow
- 3.2 Dissolved and particulate phase water quality
- 3.3 Sediment and contaminant transport

4.0 Analyze and interpret hydraulic data

5.0 Evaluate appropriate statistical, physical, hydrogeologic and contaminant transport models for comparison with existing data, particularly availability and suitability to LANL environment

6.0 Provide investigation and analysis reports as requested

ACCOMPLISHMENTS

Objective 1.0

Papers from work in Potrillo Canyon were revised for submission for publication. A seminar on approaches to modelling hydrologic transport of sediment and contaminants was given to a working group of hydrologists and geologists at LANL. The plans for instrumenting and studying the discharge sink in Potrillo Canyon were reviewed. An overall plan for the study of the hydrology and geomorphology in Big Buck Canyon were formulated.

Objective 2.0

Three tests (24 hour leaching, kinetics and total element) were conducted on samples of sediment from EF and Skunk Works sites in Potrillo Canyon. The methodology and results of these tests are presented in "Summary of Experimental Techniques" by Russell T. Herrin (copy attached). The leaching tests showed that: Ba,Ni,and U gave significant concentrations, while Be,Cd and Pb concentrations were very low or difficult to detect. Concentrations of Ba, Ni and U leached from site EF sediments were 3-6 times greater than Skunk Works concentrations; pH had a small effect; and larger masses of metals were leached from smaller sized sediments on a per gram basis. The kinetic tests showed that Ba,Ni,U concentrations increased 1.5-4 times their initial concentrations in 24-240 hours. These results are greater than those obtained by Dr. Naomi M. Becker (earlier study of sediments from these sites), as a very concentrated soil/water mixture (1/2) was used. Analysis of the digested sediment samples showed that $< 0.04\%$ of these elements was leached. The total mass of Cd, Ni, and U in these samples was analyzed by NAA (internal report by Richard J. Cashwell to John A. Hoopes, March 3,1995); results were inconclusive for Cd and Ni, while results for total U gave concentrations of 44.5 μg/g at EF and 3.22 μg/g at Skunk Works (similar to values obtained by N.M. Becker). A literature review on partitioning of Ba,Be, Pb,Hg,and U was conducted by Russell T. Herrin; a copy of that summary is attached.

Objective 3.0

Initial work on simulating water, sediment and contaminant movements was conducted using the KINEROS model. The results of this work and some portions of its continuation in another project are presented in the report "Runoff, Sediment, and Contaminant Research at Big Buck Canyon, LANL" by David C. Perry and John A. Hoopes (copy of report without appendices attached). Results of this work include the subdivision of the watershed into elements, the development of parameters for the runoff processes (e.g., area, slope, land cover, hydraulic conductivity,K, roughness coefficient,n, initial soil moisture, precipitation), sensitivity analyses to model parameters, and simulation of a large flood event in August 1991. The model is extremely sensitive to K and the initial soil moisture. Model parameters were adjusted to reproduce the results of the 1991 flood, based upon memories of water depths and area of inundation. Simulations of sediment movements have not been done (awaiting new model version and measured events for model calibration). This model is not suitable for contaminant

movement simulation in its present form; although contaminants are transported by water and sediment, the model does not track masses of water or sediment.

Objective 4.0

Field work was conducted to provide parameter values and to obtain calibration/ verification data for the modelling. Sensors and data logging equipment were installed at two locations in Big Buck Canyon (culverts 14 and 5). The quantities measured included: precipitation [tipping bucket gage]; flow [pressure sensor buried in channel (for depth) and later paddlewheel on pivoting arm (for velocity and depth) and crest stage recorder (for maximum depth)]; and sediment [pressure plate buried in channel (for scour and deposition during an event) and later bottles and chains (for suspended sediment and maximum scour depth). All data was transmitted to a Campbell 21X data logger next to each site.In addition a cumulative rain gage was installed near the canyon outlet. Other precipitation data along with climatological data were available from LANL stations and the Bandelier firetower. Several problems developed with buried pressure sensor devices; there was significant drift (due apparently to diurnal and seasonal temperature variations), and the instrument lagged (or did not respond to) a channel runoff event (as soil had to be saturated down to the sensor). Consequently the information from these sensors has provided only qualitative indications of flow events.

Direct measurements of the following channel and valley bottom parameters were made: hydraulic conductivity with Guelph permeameter; grain size distribution and porosity from soil samples; and channel morphology (cross section, slope and roughness).

Objective 5.0

Models of various types were identified and evaluated for their applicability to the LANL environment. Model characteristics and approaches to modelling are summarized in the LANL report "Hydrologic Transport and Ecosystems Investigation", LAUR-95-2800, August 1995.

Objective 6.0

Reports from this work, noted in sections above, are attached.

Sorption Characteristics of Uranium, Lead, Mercury, Barium, Beryllium, Cadmium,and Nickel: A Literature Survey

Russell T. Herrin

Introduction:

The following document represents a summary of literature on the sorption behavior of U, Pb, Hg, Ba, Be, Cd and Ni. The effects of time allowed for sorption, solution pH, cation exchange capacity of the sorbent, sorbent particle size, solution ionic strength, system temperature, soil composition and water chemistry were studied for each metal. Where information on the above parameters were found for a given metal, it is reported below.

Uranium

Time Dependence

Sheppard and Thibault (1991) completed long-term sorption experiments with uranium in columns containing an Aquic Udic Dystrochrept soil. Columns were analyzed after 1 and 4 years of contact with the atmospheric temperature and precipitation. After 1 year, nearly all of the recoverable U lay in a zone 0.04 to 0.10 m from the top of the 0.56-m soil cores. After 4 years, the maxima in the columns lay in a zone 0.14 to 0.20 m below the top of the core. Average U recovery after 4 years was 67%; the remainder was assumed to have become dispersed throughout the remainder of the column at levels below detection limits. These results led to calculated K_d values ranging from 16 to 295 L/kg for uranium. K_d values were almost an order of magnitude higher at the 1-year sampling interval than at the 4-year interval, indicating a slow desorption of uranium.

Desorption experiments were undertaken by Sheppard and Thibault (1992) on the same soil. In 90-day desorption experiments, a negligible amount (less than 5 percent) of bound U was desorbed from all soil profiles. Desorption experiments were also performed on the organic litter at the top of the soil profile; over 35 percent of the bound U was removed from this litter layer.

pH Dependence

Sheppard and Thibault (1991) found a notable, though not quantifiable, relation between soil pH and K_d; larger pH values led to lower distribution coefficients.

Results of experiments studying the dependence of sorption extent on pH were reported for Yucca mountain tuff samples by Meijer (1990). Data was taken from Thomas (1987). Experiments were performed under oxidizing conditions. K_d values ranged from 0 to 30 L/kg; most measurements were in a range from 0 to 15 L/kg. Zeolitic, devitrified and vitric tuff samples' pH-sorption characteristics were compared. A best-fit curve for K_d-pH behavior with devitrified tuff increases from K_d's of 2 to 5 L/kg at pH 6 to a maximum of 10 L/kg at pH 7.5. Beyond pH 7.5 K_d drops quickly to 0 L/kg near pH 9. Vitric tuff samples showed very similar behavior. Zeolitic samples' K_d values decrease almost linearly with pH. Distribution coefficients are in a range of 12 to 25 L/kg at pH 7 and decrease uniformly to 0 to 10 L/kg at pH 9, depending on the specific tuff sample.

A correlation appears to exist between range of K_d values at a given pH and ratio of Ca+Mg to Na+K of the clinoptilolites in tuff samples (Broxton et al., 1986). This fact, along with the pH information above, suggest that U sorbs to zeolitic tuffs primarily through an ion exchange mechanism.

Effect of Cation Exchange Capacity

No positive correlation was found between K_d and cation exchange capacity for an Aquic Udic Dystrochrept soil (Sheppard and Thibault, 1991). Similarly, tuff samples from Yucca Mountain Nevada (Daniels, et al., 1982) showed no correlation. In addition, no correlation was evident between K_d and particle surface area for Yucca Mountain tuffs.

Effect of Temperature

Tuff sorption ratios (R_d; identical to K_d, except that a state of sorption equilibrium is not implied) were determined at the Yucca Mountain, Nevada site at both 20 °C and 70 °C (Daniels, et al., 1982). R_d values were uniformly higher at 70 °C than at 20 °C. R_d values calculated from adsorption experiments were 1.6 to 5.3 times higher at 70 °C and values calculated from desorption experiments were 1.5 to 4.7 times higher at 70 °C.

Effect of Soil Composition and Water Chemistry

Sheppard and Thibault (1991) calculated K_d values for uranium in different horizons of Aquic Udic Dystrochrept (acidic sand) soil columns. Both leachate (L) and groundwater (G) cores were prepared. L cores were spiked at the top and allowed to leach as a result of precipitation infiltration. G cores were spiked at the bottom and contained a synthetic groundwater, so that capillary rise was the principal transport mechanism. The results are summarized in Table 1.

Table 1: Distribution coefficients at 1 year and 4 years for leachate and for capillary rise (groundwater) columns (Sheppard and Thibault, 1991).

Horizon	Leachate K_d (L/kg)		Groundwater K_d (L/kg)	
	1 year	4 years	1 year	4 years
Litter	--	58	--	42.6
Ae	--	295	172	26.5
Upper B	--	160	226	15.8
Lower B	19.8	45.4	70	18.3

No strong correlation between any given soil parameter and K_d could be inferred from these results; the differences in such parameters as cation exchange capacity were not large enough between horizons to allow such conclusions to be drawn.

The chemical constituents of a soil profile to which uranium principally adsorbs has been investigated by Sheppard and Thibault (1992) via sequential extractions (Tessier, et al., 1979). It was concluded that 58 to 72 percent of the U in all horizons of the Aquic Humic Dystrochrept was bound to Fe or Mn oxides. Twenty-six to 36 percent was bound to carbonates, and in any horizon, less than 8 percent of U present was readily exchangeable or bound to organics.

Adsorption experiments were completed on several different varieties of tuff from Yucca Mountain Nevada (Daniels, et al., 1982). Samples of zeolitized tuff provided sorption coefficients (R_d; identical to K_d, except that a state of sorption equilibrium is not implied) of approximately 5 L/kg. Glassy tuff samples spanned an R_d range of 0 to 20 L/kg. R_d values for clay samples were in the range of 4 L/kg, and for devitrified samples were approximately 2 L/kg.

Sheppard and Thibault (1990) surveyed available literature and developed a summary of experimentally determined K_d values for several different metals in 4 different soil types. The soil types which they defined are sand soils (soils containing ≥70 percent sand), loam soils (soils with an even distribution of sand- clay- and silt-sized particles or with ≥80 percent silt-sized particles), clay soils (soils containing ≥35 percent clay-sized particles) and organic soils (soils containing >30 percent organic matter). Their findings for U are summarized in Table 2 below.

Table 2: Distribution coefficients for uranium (L/kg) (Sheppard and Thibault, 1990)

	Sand Soil	Loam Soil	Clay Soil	Organic Soil
μ[a]	3.5	2.5	7.3	6.0
σ[b]	3.2	3.3	2.9	2.5
# observations	24	8	7	6
low value	0.03	0.2	46	33
high value	2200	4500	3.95×10^5	7350

[a] Mean of the natural logarithms of the observed values.
[b] Standard deviation of the natural logarithms of the observed values.

Clearly structural and chemical differences within a given soil type, as well as different experimental techniques, can lead

to radical differences in observed K_d values. Based on average values, it would appear that uranium K_d is directly proportional to organic matter content and to clay content.

Sorption behavior of uranium is strongly affected by solution characteristics such as pH, oxidation-reduction potential, and dissolved ion concentration. Uranium can form complexes with hydroxide ions, carbonate ions, phosphate ions and chloride ions (Matzner, 1993). In oxic groundwaters (above $E_h \approx -0.1$ V) U is in the +6 oxidation state, and is usually found as the UO_2^{2+} species, if no other complexing agents are present. The solubility of hydroxo-complexes of UO_2^{2+} is very low; the solubility has been determined to be in a range from 10^{-8} to 10^{-10} mol/l. This range is not necessarily appropriate for application to natural systems, however, since presence of complexing agents other than OH^- can strongly affect solubility (Lieser et al., 1990).

The predisposition of UO_2^{2+} to form hydroxo complexes affects its sorption behavior as well as its solubility. Sorption of U to titanium dioxide under oxic conditions was studied by Lieser et al. (1990). Maximum sorption was found to occur near pH 7. Sorption behavior with respect to pH parallels formation of the monohydroxo complex UO_2OH^+. In addition, its maximum value is very near the isoelectric point of TiOH groups. These facts point toward a surface complexation effect; UO_2^{2+} apparently forms complexes with hydroxide associated with the TiO_2 surface and is thereby sorbed to it. In systems containing large concentrations of carbonate ions, the $UO_2(CO_3)_3^{4-}$ complex may form (Stumm and Morgan, 1981), creating potential for other surface and/or soluble complexes to form.

Under anoxic conditions, uranium is in the +4 oxidation state. Uranium in this state is not as soluble as U(VI). Generally, reduction of Uranium is thought to occur when sulfide, molecular hydrogen or an organic compound is present as the reducing agent. Research has shown, however, that direct enzymatic reduction of U by bacteria can occur (Lovley et al., 1991). A sudden decrease in solubility of U could have two effects: (1) it could precipitate U in the form of flocs or large particles which would be immobile, or (2) it could precipitate U in a colloidal size range which would enhance its mobility. Similar effects with regard to a change in solvent conditions precipitating mobile colloids has been observed with other metals (Gschwend and Reynolds, 1987).

Lead

pH Dependence

Basta, et al. (1992) presented results indicating that distribution coefficients for Pb increase with increasing pH. In addition it was determined that K_d increases with decreasing initial Pb solution concentration. The lowest initial Pb concentration studied was 0.2 mM, and the highest was 5.0 mM. The results from these two concentration extremes are summarized in Table 3. K_d values are in L/kg, and the slope listed is for a linear regression of a plot of log K_d vs. pH. Values of slopes for intermediate solution concentrations did not rise uniformly; slopes increased steadily from 0.2 mM to 1.0 mM, and then decreased steadily from 1.0 mM to 5.0 mM. The maximum slope, at 1.0 mM, was 0.819.

Table 3: Distribution coefficients at given pH and Pb concentration values (Basta, et al., 1992)

Concentration (mM)	pH	log K_d	pH	log K_d	Slope
0.2	4.5	3.3	5.7	3.6	0.343
5.0	3.8	1.4	4.4	1.6	0.426

Haji-Djafari, et al. (1981), referenced in Sheppard and Sheppard (1991), studied pH dependence of Pb in a fine sandstone, silty sand. They calculated K_d values of 20, 100, 1500, and 4000 L/kg at pH 2.0, 4.5, 5.8 and 7.0, respectively. Clearly the same trend in pH-K_d relationship exists over a broader range of pH than that studied by Basta, et al.

Effect of Soil Composition and Water Chemistry

The predominant inorganic complexes formed by lead in freshwaters under aerobic conditions are $PbCO_3^0$ and $Pb(CO_3)_2^{2-}$ (Stumm and Morgan, 1981). Since most soil and aquifer particles are negatively charged, it could be assumed that little Pb sorption would occur in CO_3-rich water as a result of formation of neutral or negative complex formation. This is not necessarily true, however; Pb may undergo surface complexation with carbonate-containing solids in the aquifer matrix. In addition, Pb readily forms complexes with organic matter, making organic soils "an almost perfect sink" (Tyler, 1978, as referenced by Sheppard and Sheppard, 1991) for Pb.

Sheppard and Sheppard (1991) calculated distribution coefficients for lead between soil and porewater from soil column and field samples for several different soil types. Their findings are summarized in Table 4. Distribution coefficients

shown represent the geometric mean of values from all experiments. The sand is a boreal acidic sand, the peats are boreal acidic organic soils, and the loams are agricultural soils.

Table 4: Distribution coefficients and pH values for different soil types (Sheppard and Sheppard, 1991).

Soil Type	Soil pH	K_d (L/kg)
Brunisol Sand	4.9	19
Sedge Peat	5.5	3×10^4
Sphagnum Peat	4.8	9000
Luvisol Loams	7.0	$>6 \times 10^4$
Luvisol Clay Loam	7.0	$>6 \times 10^4$
Gleysol Loam	7.3	2.1×10^4

In the Aquic Udic Dystrochrept (acidic sand) studied by Sheppard and Thibault (1992), over 70 percent of adsorbed Pb was sorbed to Fe and Mn oxides. The organic matter in the upper portion of the A-horizon bound 9.3 percent of the Pb included in it. In the B-horizon, 15.2 percent was bound to carbonates. Organic carbon content was at least an order of magnitude higher in the upper portion of the A horizon than in any other part of the soil profile, which may explain the unusually large amounts of Pb bound to organic matter in this layer.

Using the Techniques of Tessier, et al. (1979), Xian et al. (1989) completed desorption experiments similar to those of Sheppard and Thibault. Xian et al. used two different surface loams and one sandy loam. In these soils, Fe- and Mn-bound oxides did not dominate other fractions as in the acidic sand of Sheppard and Thibault. Little Pb was exchangeable or bound to carbonates, as was the case in Sheppard and Thibault's study. Fraction bound to organic carbon, however, was much greater in the loams studied. In one surface loam, approximately 30 percent of extractable Pb was bound to the organic fraction, while approximately 40 percent was bound to Fe-Mn oxides. In the other two soils, twice as much was bound to the organic fraction as was bound to the Fe-Mn oxides. In these soils the amount in the residual fraction -- indicating the strongest sorption -- was similar in magnitude to the amount bound to the Fe-Mn oxides. The large percentage of Pb bound to organic carbon cannot be explained by soil organic carbon content; organic carbon levels in all horizons of Sheppard and Thibault's sand were at least two orders of magnitude higher than the highest levels in the soils of Xian, et al. Neither group performed tests to determine the

character of the organic carbon present. Schuster (1991) pointed out that Hg was more strongly bound to organic material with a high sulfur content; in similar fashion, Pb may sorb differently to different types of organic matter.

In sorption studies on 11 soils, Buchter, et al. (1989) calculated that Pb K_d and exchangeable hydroxide content were correlated at the 0.01 probability level ($r = 0.907$). Lead K_d and aluminum oxide (Al_2O_3) content were also correlated at the 0.01 probability level ($r = 0.908$). The amorphous iron oxide (Fe_2O_3) content of the soil was correlated to K_d at the 0.05 probability level ($r = 0.759$). The K_d for Pb was not significantly correlated to pH, total organic carbon content, cation exchange capicity, manganese oxide content, free iron oxide, or sand, silt or clay content. The pattern of correlation to the Freundlich n parameter was the same; in fact r values for the three significantly correlated parameters were slightly higher for the n than for K_d.

Sheppard and Thibault (1990) compiled literature K_d values for metals including Pb. The results are shown in Table 5 below.

Table 5: Distribution coefficients for lead (L/kg) (Sheppard and Thibault, 1990)

	Sand Soil	Loam Soil	Clay Soil[c]	Organic Soil
μ[a]	5.6	9.7	6.3	10.0
σ[b]	2.3	1.4		0.5
# observations	3	3		6
low value	19	3500		9000
high value	1405	59,000		31,590

[a] Mean of the natural logarithms of the observed values.
[b] Standard deviation of the natural logarithms of the observed values.
[c] Value estimated from soil:plant concentration ratio

These somewhat broad-ranging results show that structural and chemical variation within a soil type, as well as differences in experimental technique can greatly affect K_d values. Trends are difficult to define, particularly if the clay soil estimate is not considered trustworthy. The sand and loam results indicate that particle size may be an important factor.

Mercury

Time Dependence

The kinetics of mercury sorption were studied by Nyffeler, et al. (1984) using seawater and surface sediments from Narragansett Bay in batch-type experiments. The first distribution coefficient measurement, taken less than 1 day after the batch sample was spiked, gave a value of 9×10^4 L/kg. The K_d value then increased to a value of approximately 1.8×10^5 L/kg, approximately 3 days after spiking. The K_d was next determined 50 days after sample spike, at which time its value was identical to that at the 3 day sampling.

pH Dependence

Barrow and Cox (1992), studied the effect of pH on Hg sorption to a loamy sand both in the presence and absence of chloride ion. Soil pH values were adjusted to a range of values between 4 and 7. In the absence of chloride, little change in the sorptive behavior of Hg was detected between pH values of 4 and 6. Between pH 6 and 7, however, the sorbed Hg level dropped from approximately 4 μmol/g to 2 μmol/g. With a chloride concentration of 10^{-4} M, sorption levels were much lower than in chloride-free solutions; at a pH of 4, sorption was approximately 0.3 μmol/g. Sorption values in this 10^{-4} M solution rose steadily to a value near 3 μmol/g at pH 6, and then descended to 2 μmol/g at pH 7.

Effect of Soil Composition and Water Chemistry

Sorption behavior of sediments taken from three different depths at the Idaho Chemical Processing Plant was studied by Del Debbio (1991). Alluvium (a sandy loam), interbed sediment (a silt) and basalt taken from, respectively, 12 m, 35 m and 40 m below land surface were each tested in batch experiments with Hg. Sorption at different Hg concentrations were studied, and the resulting data were fit to Freundlich isotherms, described by the equation

$$S_m = kC_e^n$$

where S_m = moles of solute sorbed/g of soil
C_e = equilibrium solute concentration, mol/l
k and n = constants.

Table 6 presents the range of Hg concentrations studied, the resulting K_d values, and the Freundlich constants calculated.

Table 6: Mercury sorption parameters (Del Debbio, 1991).

Geologic Material	Initial Concentration (M)	Measured K_d (L/kg)	Freundlich Constants	
			k (L/kg)	n
Interbed Sediment	6.5×10^{-7}- 1.0×10^{-5}	998-80.8	0.109	0.49
Alluvium	3.3×10^{-7}- 1.0×10^{-5}	1910-236	1.89	0.64
Basalt	6.9×10^{-7}- 1.0×10^{-5}	171-9.54	not listed (poor fit)	not listed (poor fit)

Over an initial Hg concentration range from 0.25 to 20 ppm, Ramamoorthy and Rust (1978) found that sorption to sandy, silty and organic-rich river sediments were well-fitted to the linear form of the Langmuir equation:

$$C/x/m = (1/kb) + C/b$$

Where: C = equilibrium concentration of sorbent
x/m = amount of sorbate per unit mass sorbent
k = constant related to bonding energy
b = sorption maximum.

Correlation coefficients describing the fit of the Langmuir equation to experimental data were almost all greater than 0.9.

It is not immediately clear why Del Debbio and Ramamoorthy and Rust found good correlation to completely different sorption equations. The metal concentration range studied by Del Debbio was about an order of magnitude lower than that studied by Ramamoorthy and Rust; this may be a factor. Another possible factor is the different characters of the sediments that the two groups studied.

Redox conditions and availability of ligands can both modify the sorptive behavior of Hg. The two oxidation states of Hg which are most important in soil and groundwater conditions are Hg^0 and Hg^{2+}. Under mildly oxidizing conditions above pH 5, most Hg is in the form of Hg^0. Over a broad range of conditions, the solubility of Hg^0 is about 56 ng/g. Under more reducing conditions, Hg is principally in the form of HgS, with a solubility of only 0.002 ng/g. The propensity of Hg for S also causes it to sorb preferentially to dissolved organics or organic coatings with S-containing functional groups (Schuster, 1991).

Only in well-oxygenated environments, such as those normally present in soils, do high solubilities of Hg occur. In basic systems, Hg is principally in the form of $Hg(OH)_2^0$; under acidic conditions, $HgCl_2^0$ predominates (Schuster, 1991). HgClOH serves as a transition complexe, dominating near pH 7. The dominance of

these uncharged complexes does not prevent binding to soil, however; in fact under a broad range of conditions, a much higher fraction of Hg is bound to soil solids than is present in associated porewater. This is largely a result of surface complexation; Hg complexes with OH, Cl and other functional groups on soil solids. This type of sorption is much more stable than sorption resulting from ion exchange (Schuster, 1991).

Barium

Time Dependence

Results of kinetics experiments using barium in a Narragansett Bay surface sediment and seawater system were reported by Nyffeler, et al. (1984). Similar experiments were run using sediments from San Clemente Basin and MANOP site H.

Nearly all sorption to Narragansett Bay sediments occurred within the first two days after spiking with barium. In this time the distribution ratio increased from 5 L/kg to 20 L/kg. It remained between 20 and 30 L/kg for the remainder of the experiment, or 109 days. San Clemente Basin sediments showed the least difference with time; distribution ratios rose from 25 to 30 L/kg in the first two days, and then slowly dropped back to near 25 in the following 48 days. Time had the most dramatic effect on MANOP site H sediments, wherein distribution ratios rose from 250 L/kg to 10,000 L/kg in the first 10 days, and continued to rise to a value of 20,000 L/kg at 30 days. The MANOP site H experiment was halted at 30 days, but Ba sorption appeared as if it would continue to increase after this time. Nyffeler, et al. suggest that the much greater sorption of Ba to MANOP site H sediments may be a result of ion exchange between Ba and Mn; Mn levels are much higher in MANOP sediments than in the other two, and are likely in the form of MnO_2 coatings on the sediment particles.

Eylem, et al. (1989) determined that Ba reached equilibrium sorption levels in a chlorite-synthetic groundwater batch system in approximately 6 days.

Effect of Cation Exchange Capacity

Experiments performed on Tuff samples from Yucca Mountain, Nevada (Daniels, et al., 1982) indicated a positive correlation existed between cation exchange capacity and sorption ratio.

Effect of Particle Size

Daniels, et al. (1982) calculated sorption ratios for tuff particles smaller than 38 μm that were 2 to 5 times higher than for particles larger than 38 μm. The <38 μm fraction, however, had a higher clay content than the >38 μm fraction; this increased clay content may have had a greater effect on sorption than did particle size.

Effect of Temperature

Experiments on Yucca Mountain, Nevada tuff samples (Daniels, et al., 1982) were performed on batch samples held at both 20°C ±

4°C and at 70°C. These experiments indicate that Ba sorption ratios are 2 to 5 times higher at the higher temperature.

Effect of Soil Composition and Water Chemistry

Stumm and Morgan (1981) indicate that barium does not form complexes in freshwaters under aerobic conditions to any significant degree. Its principal dissolved species under these conditions is Ba^{2+}. As a result, Ba is not likely to form surface complexes with CO_3^{2-} or OH^- functional groups on aquifer solids. Barium ions should, however, be electrostatically attracted to aquifer solids, which generally are negatively charged. Strength of sorption due to electrostatic interactions is strongly affected by parameters which can modify the electric double layer thickness surrounding particles. Such effects include particle geochemistry and solution ionic strength (McDowell-Boyer, 1992).

Sorption of Ba to 3 clay types -- kaolinite, montmorillonite and chlorite -- was studied by Eylem, et al. (1989). Batch experiments were performed using synthetic groundwater of a similar composition to the groundwater in the regions where the clay was sampled. Adequate time was allowed for equilibrium to be attained before K_d values were determined. Barium provided a K_d of 127 L/kg with kaolinite, 238 L/kg with montmorillonite and 745 L/kg with chlorite. Eylem and co-workers felt that these sorption values were sufficiently close to one another to merit no real analysis of the cause of the small differences. It was, however, determined that no correlation existed between cation exchange capacity of the clays and final K_d.

Grutter and co-workers (1992) performed batch sorption experiments on chlorite, montmorillonite and illite. In addition, experiments were performed on a glaciofluvial material. A synthetic groundwater was used as the liquid phase. Barium was spiked into batch samples at concentrations ranging from 2.5×10^{-8} M to 1.0×10^{-4} M. The range of log K_d values (referred to as log R_d values by Grutter et al.) are compiled in Table 7. The logarithmic values are taken from R_d values in L/kg.

Table 7: Barium distribution ratios for different mineral types (Grutter et al., 1992)

Mineral	log R_d (low value)	log R_d (high value)
Montmorillonite	2.3	2.4
Illite	2.1	3.0
<40 μm Chlorite	1.2	2.5
< 2 μm Chlorite	2.8	4.0
<32 μm Glaciofluvial Mat.	1.5	3.1

Grutter's and Eylem's calculated barium K_d's for montmorillonite and chlorite systems are very comparable. The majority of chlorite in samples studied by Eylem et al. fell in a particle size range between 2 μm and 32 μm, and their K_d estimate fell at the very low end of the K_d range described by Grutter et al. for <2 μm chlorite.

Grutter saw a definite correlation between K_d and cation exchange capacity for modified glaciofluvial materials. Treatments were performed on different samples of glaciofluvial material such that: (1) exchangeable Ba, Sr, and other interfering cations were removed; (2) carbonates were removed; (3) Fe and Mn oxides were removed; and (4) organic substances were removed. Sorption experiments were performed these modified materials and R_d values calculated for each. Normalizing the R_d values using cation exchange capacity brought R_d-concentration curves much closer together than non-normalized curves, indicating that the principal effect of the modifications described above was due to change in cation exchange capacity. The data of Daniels, et al. (1982) also indicated a correlation between R_d and cation exchange capacity.

Tuff samples of different morphology from the Yucca Mountain, Nevada site showed notably different sorption characteristics for barium (Daniels, et al., 1982). A strong correlation was found between R_d and zeolite content. Samples with higher zeolite content sorbed barium to a much greater extent than samples with low zeolite content. Daniels and co-workers attributed this effect to the high cation exchange capacity of zeolites in conjunction with the simplicity of the Ba cation. Glassy samples and devitrified samples with zeolite contents less than 10 percent had similar R_d values with respect to Ba.

Beryllium

Time Dependence

Sorption of beryllium with time was studied by You, et al. in systems with solid phases of illite, montmorillonite, and bauxite soil. Samples with river water and with seawater for the liquid phase were studied. The behavior of illite, bauxite and montmorillonite in river water was qualitatively quite similar. Measured K_d values rose quickly in the first day; log K_d values rose by approximately 0.75. Values rose much more slowly after this point. The difference between the 2-day and 20-day log K_d values was between 0.5 and 0.75, and the difference between the 10-day and 20 day K_d values were almost undetectable on a log K_d-time plot.

Seawater samples rose much more slowly in the first 5 days. In the illite and bauxite systems, seawater and river water values became nearly identical from 5 to 20 days. In the case of montmorillonite, the K_d values for seawater were always significantly lower. At 20 days, river water samples were at a K_d of 5.3 while seawater samples were at a K_d of 4.75.

pH Dependence

You, et al. (1989) saw a very strong K_d-pH relationship for beryllium, particularly at low pH. River water was used as the liquid phase in all pH experiments. The 3 different solid phases on which pH experiments were performed (kaolinite, illite and river mud) provided identical results, within experimental error. Near a pH of zero, log K_d values were near 1.0. Values rose quickly with pH (K_d increase was particularly strong near pH 5) until log K_d's of 5.5 to 6.0 were reached at a pH of 8. Values of log K_d then decreased slightly until they reached the 4.5 to 5.0 range at a pH of approximately 13. It was noted that pH dependence of Be K_d was the strongest relationship determined and was essentially independent of particle type. In addition, You and co-workers' pH-K_d relationship was similar to that determined by Bloom and Cornelius (1983) in a seawater system. This indicates that the pH-K_d relationship is not strongly affected by solution ionic strength.

You, et al. pointed out that the pH dependence of K_d for Be is similar to the pH dependence of the solubility of hydroxides (e.g., $Al(OH)_3$, $Fe(OH)_3$). This may indicate that Be sorption is tied to hydroxide solubility.

The general trend of the above findings is supported by the work of Vesely, et al. (1989). In their study, stream waters were sampled, and their average pH values were compared to Be concentration. A definite negative correlation was found between pH and Be concentration, indicating that at low pH, more Be was sorbed to immobile solids.

Effect of Temperature

You, et al. (1982) studied a river mud-river water-beryllium system at both 25°C and 60°C. Temperature had a strong, positive effect on sorption. Distribution coefficients for 60°C systems were as much as an order of magnitude higher and never less than 5.8 times higher over the 20 days during which measurements were made.

Effect of Soil Composition and Water Chemistry

The predominant dissolved form of beryllium in aerobic freshwaters is $Be(OH)^+$ (Stumm and Morgan, 1981). A positively-charged hydroxyl species is likely to bind effectively to many solid substances. Surface complexation can take place to solids with OH^- functional groups on their surface, and the positive charge of the complex will create electrostatic attraction to negatively-charged soil and aquifer particles.

Sheppard and Thibault (1990) used soil:plant concentration ratios to predict beryllium K_d's in three different types of soil. In sand soil, K_d was estimated at 250 L/kg. In loam soil, the K_d estimate was 800 L/kg. In Clay soil, K_d was estimated at 1300 L/kg. In organic soil, the approximate K_d was 3000 L/kg. Sheppard and Thibault found no experimental partitioning values in the literature to which these concentration ratio estimates could be compared.

Extensive sorption tests under varied conditions were undertaken by You, et al. (1989). Sorption for several different solid types in a river water solution (pH = 7.8, salinity < 3 per mil, solid concentration 0.2 g/l) showed that Be sorbs very strongly to many different mineral types; K_d values ranged from 4.4×10^4 to 1.2×10^6, except for beryl. The results for the different minerals tested are summarized in Table 8. The mud studied was from a lake bed. The silt was from a riverbed and were composed of quartz, feldspar, calcite and clay minerals. The bauxite soil is a weathered andesite the major components of which are gibbsite, quartz, illite, kaolinite and hematite.

Further tests performed by You, et al. indicated that dissolved organic matter has little effect on beryllium K_d. In direct contradiction to this finding, the study of Vesely, et al. (1989) produced results indicating that Be is "significantly bound" to natural organic substances, particularly low molecular weight organics (e.g., fulvic substances).

Table 8: Results of Be K_d batch experiments (You, et al., 1989)

Solid Mineral	K_d (L/kg)
Man-made:	
δ-MnO_2	1.2×10^6
BeO	2.4×10^5
Natural Samples:	
Bauxite	1.1×10^6
Mud	1.2×10^5
Silt	9.0×10^4
Sand	1.0×10^5
Minerals:	
Illite	2.2×10^5
Montmorillonite	2.1×10^5
Kaolinite	1.6×10^5
Calcite	9.5×10^4
Dolomite	4.5×10^4
Talc	4.4×10^4
Beryl	3.5×10^3

Cadmium

Time Dependence

pH Dependence

Basta, et al. studied K_d dependence on pH. Batch samples used in the study contained 1 g of Galva silt loam and 25 ml of 10 mM $Ca(ClO_4)_2$ aqueous solution containing a known concentration of Cd. Different samples were adjusted to different pH values with $HClO_4$ or NaOH.

The results of Basta's study showed that the K_d of a cadmium-water systems is directly related to pH (over the range studied) and inversely proportional to the metal concentration in solution. Table 9 gives K_d's at the lowest and highest pH values studied for each initial metal concentration. From Table 9 it can be seen that slope decreases as concentration increases; pH dependence of K_d decreases with increasing concentration.

Table 9: Distribution coefficients at given pH and Pb concentration values (Basta, et al., 1992)

Concentration (mM)	pH	log K_d	pH	log K_d	Slope
0.2	4.7	1.4	5.8	1.8	0.366
1.0	4.6	1.1	5.6	1.5	0.313
2.0	4.5	0.9	5.8	1.8	0.274

Mann and Ritchie (1993) studied the effect of pH (over a range of 4 to 7) on the extent of Cd sorption to different soil fractions. Their extraction techniques are similar to those of Tessier (1979). Four soils were studied which differed in their clay, hydrous oxide and organic matter content. The amount of Cd in the exchangeable fraction was always large in siliceous sands, and increased with increasing pH. In peaty sands increasing pH led to greater sorption by the organic fraction, until at pH 7 60 percent of the Cd was bound to the organic fraction. In soils dominated by hydrous oxides (principally goethite), the majority of Cd was bound to oxides and to the residual fraction. Amounts bound to both of these fractions increased with increasing pH. High clay-content soils retained Cd mainly in the exchangeable forms at all pH values, though more was bound to residual and organic fractions at higher pH values.

In their study of 11 different soils, Buchter, et al. (1989) found that Cd K_d values were correlated with pH at the 0.05 probability level ($r = 0.666$). A significant negative correlation (significance at the 0.01 probablility level, $r = -0.942$) was found between Cd K_d of the different soils and the

Freundlich n parameter. No adjustment of pH was performed on the different soils; correlation was performed using the native pH of each of the 11 soils.

Effect of Cation Exchange Capacity

Buchter, et al. (1989) also determined, via their study of 11 soils, that Cd sorption was correlated to cation exchange capacity at the 0.01 probability level ($r = 0.740$). Correlation of CEC with the Freundlich n parameters for Cd with the different soils was not significant, however.

Effect of Soil Type and Water Chemistry

Cadmium dissolved in oxic fresh water is likely to be in one of two forms: Cd^{2+} or $Cd(OH)^{+}$. In aerobic seawater, $CdCl_2^0$ dominates. The abundance of negatively-charged solids and solids containing OH^- functional groups in aquifer matrices point toward a high degree of sorption of Cd to these solids.

Sheppard and Thibault (1990) compiled literature K_d values for Cd for 4 different soil types. The results of this compilation are summarized in Table 10.

Sorption behavior of sediments taken from three different depths at the Idaho Chemical Processing Plant was studied by Del Debbio (1991). Alluvium (a sandy loam), interbed sediment (a silt) and basalt taken from, respectively, 12 m, 35 m and 40 m below land surface were each tested in batch experiments with Cd. Sorption at different Cd concentrations were studied, and the resulting data were fit to Freundlich isotherms, described by the equation

$$S_m = kC_e^n$$

where S_m = moles of solute sorbed/g of soil
C_e = equilibrium solute concentration, mol/l
k and n = constants.

Table 10: Distribution coefficients for cadmium (L/kg) (Sheppard and Thibault, 1990)

	Sand Soil	Loam Soil	Clay Soil	Organic Soil
μ^a	4.3	3.7	6.3	6.7
σ^b	1.5	1.6	0.9	2.3
# observations	14	8	10	9
low value	2.7	7.0	112	23
high value	625	962	2450	1.7×10^4

[a] Mean of the natural logarithms of the observed values.
[b] Standard deviation of the natural logarithms of the observed values.

Table 11 presents the range of Cd concentrations studied, the resulting K_d values, and the Freundlich constants calculated. The exponential Freundlich parameters (n values) calculated for interbed sediment and alluvium are close to 1. This indicates that sorption isotherms for Cd with these two sediment types are nearly linear.

Table 11: Cadmium sorption parameter ranges (Del Debbio, 1991).

Geologic Material	Initial Concentration (M)	Measured K_d (L/kg)	Freundlich Constants	
			k (L/kg)	n
Interbed Sediment	3.7×10^{-9}- 1.5×10^{-6}	1.69×10^4- 1.39×10^4	1000	0.88
Alluvium	3.7×10^{-9}- 1.5×10^{-6}	6410-4430	4360	0.99
Basalt	3.7×10^{-9}- 1.5×10^{-6}	3590-1300	not listed (poor fit)	not listed (poor fit)

Nickel

Effect of pH

The distribution coefficient for Ni increases with increasing pH and with decreasing concentration. Furthermore, extent of change in K_d with pH change increases with decreasing concentration. Slope of a graph of log K_d versus pH dropped from 0.364 to 0.180 as initial Ni solution concentration rose from 0.2 mM to 2.0 mM. At 0.2 mM Ni, log K_d values increased from 1.3 to 1.8 over a pH range from 4.5 to 6.0. At 2.0 mM Ni, log K_d increased from 1.1 to 1.3 over a pH range from 4.5 to 6.0 (Basta et al., 1992).

Effect of Soil Type and Water Chemistry

Stumm and Morgan (1982) list the probable dissolved inorganic species of Ni as Ni^{2+} and $NiCO_3^0$. Stumm and Morgan point out that the carbonate complex of Ni may not form to a significant degree. If its formation is in fact extensive, surface complexation of Ni to carbonate-containing solids could be an important sorption mechanism. If its formation is extremely limited, then electrostatic interaction will be the only important sorption mechanism in aquifers.

Nickel is also complexed by organic matter. Warwick and Hall (1992) undertook a study of nickel complexation by a moorland water containing humic and fulvic substances, as well as on a purified humic acid sample. The results were used to calculate K values as defined by the equation

$$K = [ML] / ([M]([ML]_{max} - [ML]))$$

Where $[ML]$ = concentration of metal bound to organics
$[M]$ = concentration of unbound metal
$[ML]_{max}$ = maximum complexing capacity of the organics.

The average Log K value for the natural water was 4.40, and the average Log K for the pure humics was 4.10. The difference between these values was not statistically significant. These high Log K values indicate that a significant amount of dissolved Ni will be complexed by dissolved organics or to organic coatings on aquifer particles.

A compilation of literature distribution coefficients for metals under oxic conditions was prepared by Sheppard and Thibault (1990) for four different soil types. Nickel K_d values were collected and averaged for sand, clay and organic soils, and were estimated using soil-to-plant concentration ratios for loam soil. K_d values for Ni were more similar between soils than those for other metals. In addition, the range of K_d values compiled for a given soil were relatively small for Ni, usually representing only an order of magnitude. Average organic soil K_d

was the highest, with a value of 1100 L/kg. The average K_d for clay was 650 L/kg, and the average for sandy soil was 400 L/kg. The K_d estimate for loam soil was 300 L/kg (Sheppard and Thibault, 1990).

Sorption experiments were performed on soils using several different metals, including nickel, by Buchter et al. (1989). Based on these tests, the statistical significance of different soil parameters on sorption was determined. The only parameters which Buchter and co-workers found to be significant for Ni were pH and cation exchange capacity. Soil pH was positively correlated with log K_d to the 0.05 probability level, and CEC was correlated with log K_d to the 0.01 probability level. Soil pH was negatively correlated with the Freundlich n parameter to the 0.01 probability level, but CEC was not significantly correlated with the n parameter at all.

References

Barrow, N.J., and V.C. Cox. 1992. The effects of pH and chloride concentration on mercury sorption. II. By a soil. Journal of Soil Science 43:305-312.

Basta, N.T. and M.A. Tabatabai. 1992. Effect of cropping systems on adsorption of metals by soils: II. effect of pH. Soil Science 153:195-204.

Bloom, N., and E.A. Crecelius. 1983. Solubility behavior of atmospheric ^{7}Be in the marine environment. Mar. Chem. 12:323-325.

Buchter, B., B. Davidoff, M.C. Amacher, C. Hinz, I.K. Iskandar, and H.M. Selim. 1989. Correlation of Freundlich K_d and n retention parameters with soils and elements. Soil Science 148:370-379.

Daniels, W.R., K. Wolfsberg, R.S. Rundberg, A.E. Ogard, J.F. Kerrisk, C.J. Duffy, et al. 1982. Summary report on the geochemistry of Yucca Mountain and environs. Los Alamos National Laboratory report LA-9328-MS.

Del Debbio, J.A. 1991. Sorption of strontium, selenium, cadmium and mercury in soil. Radiochim. Acta 52/53:181-186.

Eylem, C., N.E. Erten, and H. Gokturk. 1989. Sorption of barium on kaolinite, montmorillonite and chlorite. Analyst 114:351-353.

Grutter, A., H.R. von Gunten, and E. Rossler. 1992. Sorption of barium on unconsolidated glaciofluvial deposits and clay minerals. Radiochim. Acta 58/59:259-265.

Gschwend, P.M., and M.D. Reynolds. 1987. Monodisperse ferrous phosphate colloids in an anoxic groundwater plume. Journal of Contaminant Hydrology 1:309-327.

Haji-Djafari, S., P.E. Antommaria, and H.L. Crouse. 1981. Attenuation of radionuclides and toxic elements by in situ soils at a uranium tailings pond in central Wyoming. in: Zimmie, T.F. and C.O. Riggs, eds., Permeability and Groundwater Contaminant Transport, ASTM STP 746, American Society for Testing and Materials, pp. 221-242.

Lieser, K.H., R. Hill, U. Muhlenweg, R.N. Singh, Tu Shu-De, T. Steinkopff. 1991. Actinides in the environment. Journal of Radioanalytical and Nuclear Chemistry 147:117-131.

Lovley, D.R., E.J.P. Phillips, Y.A. Gorby, and E.R. Landa. 1991. Microbial reduction of Uranium. Nature 350:413-416.

Mann, S.S., and G.S.P. Ritchie. 1993. The influence of pH on the forms of cadmium in four west Australian soils. Aust. J. Soil Res. 31:255-270.

McDowell-Boyer, L.M. 1992. Chemical mobilization of micron-sized particles in saturated porous media under steady flow conditions. Environ. Sci. Tech. 26:586-593.

Meijer, A. 1990. A strategy for the derivation and use of sorption coefficients in performance assessment calculations for the Yucca Mountain site in Proceedings of the DOE/ Yucca Mountain Site Characterization Project Radionuclide Adsorption Workshop at Los Alamos National Laboratory. Los Alamos National Laboratory Report LA-12325-C.

Nyffeler, U.P., Y.H. Li, and P.H. Santschi. 1984. A kinetic approach to describe trace-element distribution between particles and solution in natural aquatic systems. Geochim. Cosmichim. Acta 48:1513-1522.

Schuster, E. 1991. The behavior of mercury in the soil with special emphasis on complexation and adsorption processes -- a review of the literature. Water, Air and Soil Pollution 56:667-680.

Sheppard, M.I., and D.H. Thibault. 1990. Default soil solid/liquid partition coefficients, K_ds, for four major soil types: a compendium. Health Physics 59:471-482.

Sheppard, M.I., and D.H. Thibault. 1991. A four-year mobility study of selected trace elements and heavy metals. J. Environ. Qual. 20:101-114.

Sheppard, M.I., and D.H. Thibault. 1992. Desorption and extraction of selected heavy metals from soils. Soil Sci. Soc. Am. J. 56:415-423.

Sheppard, S.C., and M.I. Sheppard. 1991. Lead in boreal soils and food plants. Water, Air, and Soil Pollution 57/58:79-91.

Stumm, Werner and James J. Morgan. 1981. **Aquatic Chemistry, 2nd edition.** John Wiley and Sons, New York.

Tessier, A., P.G.C. Campbell, and M. Bisson. 1979. Sequential extraction procedure for the speciation of particulate trace metals. Anal. Chem. 51:844-851.

Thomas, K.W. 1987. Summary of sorption measurements performed with Yucca Mountain, Nevada, tuff samples and water from well J-13. Los Alamos National Laboratory Report LA-10960-MS.

Vesely, J., P. Benes and K. Sevcik. 1989. Occurrence and speciation of beryllium in acidified freshwaters. Wat. Res. 23:711-717.

Xian, X., and G.I. Shokohifard. 1989. Effect of pH on chemical forms and plant availability of cadmium, zinc and lead in polluted soils. Water, Air, and Soil Pollution 45:265-273.

You, C.F., T. Lee, and Y.H. Li. 1989. The partition of Be between soil and water. Chem. Geol. 77:105-118.

Summary of Experimental Techniques
Los Alamos National Laboratories
Sediment Leaching Project

Russell T. Herrin

Experimental Objectives:

Leaching characteristics of two sediments from Los Alamos National Laboratories were to be tested; one sediment is from site E-F and the other is from Skunk Works. Leaching behavior with respect to six different metals (U, Pb, Cd, Ba, Be and Ni) is to be analyzed. In addition, samples of the sediment itself are to be digested, and the digestates are to be analyzed for these metals.

Methods and Materials:

Leaching Solutions:

Solutions added to soils for leaching experiments were composed of ultra-pure (Milli-Q, Millipore Inc.) water in which the pH was adjusted with Fisher Tracemetal grade HNO_3 or with NaOH, whichever was appropriate. Two pH values were chosen: near the average sediment pH (6.8) and near average rainwater pH (4.9).

Sediment Preparation:

Sediment was oven-dried to a constant weight at 40 °C. Drying was performed either in an acid-cleaned (see below) jar or in the bag into which it was initially collected. Larger aggregates were broken up with a glass stirring rod if the sediment was in a glass jar, or by crushing them through the bag by hand if sediment was dried in a bag.

Two size separations were performed by manually agitating sediment in sieve trays. Sediment was first sieved through a #10 plastic sieve. The fraction which remained in this sieve was weighed and discarded. The fraction which went through the sieve was then put through a #200 plastic sieve. Both the retentate fraction and the pan fraction were weighed and saved in plastic bags.

Container Preparation:

Bottles in which solutions and leachate samples were stored and in which leaching experiments were performed were composed of low-density polyethylene (LDPE). Bottles were put through a two-step acid cleaning process. Bottles were first filled with a 30 percent aqueous solution of reagent grade HNO_3. This acid remained in the bottles for at least 24 hours. The 30 percent acid was reused. After 24 hours the 30 percent solution was removed. Bottles were rinsed with Milli-Q water and then filled with a 2 percent solution of Fisher Tracemetal grade acid. This acid was left in the bottles for at

least 24 hours. It was then removed (and not reused), and bottles were rinsed with ultra-pure water and left loosely capped to dry.

Twenty-Four Hour Leaching Experiments:

To determine the effects which sediment particle size, pH and sediment type have upon leaching of the elements of interest, leaching experiments were performed on Skunk works and site E-F sediments at two different pH values and on three site E-F samples: the pan fraction, the fraction which went through the #10 sieve but was retained on the #200 sieve, and sediment which was undifferentiated with respect to size.

Between 29 and 31 g of sediment were placed in a 120-ml LDPE bottle, to which 59 to 63 g of pH-adjusted Milli-Q was then added. In addition, an empty bottle was filled with each of the two types of pH-adjusted Milli-Q to be used as a control.

Samples were placed in an incubator shaker and agitated at 25 °C for 22-26 hours. They were then removed, allowed to settle for approximately 15 minutes, and decanted into 40-ml polycarbonate centrifuge tubes (the tubes had been acid cleaned using the procedure above). Samples were centrifuged at 15,000 RPM and 25 °C for 30 minutes. Centrifugate was vacuum-aspirated through a 0.05 µm polycarbonate filter (Poretics, Inc.). The filtration apparatus used was made entirely of plastic, and had been acid cleaned. Filtrate was captured directly into acid-cleaned LDPE bottles, and were immediately acidified with 100 µl concentrated Ultrex HNO_3. They were tightly capped and refrigerated to reduce evaporation effects. Sediment-free controls were centrifuged, filtered, acidified and stored by the same methods as sediment-containing samples.

It should be noted that the use of 0.05 µm filters in separation of the solid phase from the liquid phase removed not only particulate (greater than 0.45 µm) material, but in addition removed the majority of colloidal material. This study therefore represents an analysis only of dissolved material leached from sediments.

Kinetics Experiments:

To assess the effect of time on element leaching, kinetics tests were performed. To a 500-ml LDPE bottle, 199-200 g of undifferentiated sediment was mixed with 399-400 g pH-adjusted Milli-Q. In addition, an empty bottle was filled with 399-400 ml of each type of pH-adjusted Milli-Q to use as a control.

Samples were placed in the incubator-shaker at 25 °C. Aliquots were removed for analysis 1 hour, 1 day, 3 days, 7 days and 10 days after sediment and solution were mixed. Sample treatments (i.e., decanting, centrifugation, filtration, acidification and storage) were similar to those described for size fractionation experiments.

Sediment Digestions:

Sediment digestions were performed in teflon digestion bombs designed for use

in a microwave oven. The procedure outlined below is based on an established technique (Walker, M.T. 1994. Levels and Forms of Trace Metals in Wisconsin Stream Bed Sediments. M.S. Thesis, University of Wisconsin-Madison).

Approximately 200 mg of sediment was weighed into a clean, dry, tared bomb. Seven ml of Ultrex HNO_3 and 1 ml of trace metal grade HF were pipetted into the bomb. Bombs were wrench-tightened and treated by the following procedure:

a) heat 5 minutes at 20% power
b) 10 minutes cool down
c) heat 2 minutes at 80% power
d) 10 minutes cool down
e) heat 1 minute at 100% power.
f) cool to room temperature
g) add 1 ml saturated H_3BO_3 solution
h) heat 5 minutes at 20% power
i) cool to room temperature
j) dilute with ultra-pure water, and filter through a 1-μm polycarbonate filter into a clean polyethylene bottle
k) rinse bomb twice more with ultra-pure water; pour rinsate through filter into same bottle. Total volume should be approximately 60 g.

Pre-digestion bomb cleaning was accomplished by adding 7 ml trace metal grade HNO_3 to bombs and then heating them as in steps (a) through (f) above.

Saturated H_3BO_3 solution was created by adding approximately 6.7 grams of solid H_3BO_3 to 100 ml ultra-pure water, gently heating until all solid dissolved, cooling to room temperature, and decanting the resulting solution into a clean polyethylene bottle.

Results and Discussion:

Results of all 24-hour leaching experiments are summarized in Table 1. Three sediment size fractions were tested: that which was not retained on a #200 sieve (Pan), that which was retained on a #200 sieve but not on a #10 sieve (Mid), and sediment undifferentiated with respect to size (Undiff.). Tests were also conducted at two different pH values: 6.8 and 4.9. Mass of element leached per mass sediment was calculated based on concentrations of elements in leachate solutions determined by ICP-MS, and measured mass of sediment and leaching solution. Concentration results have been corrected using method blanks. The standard deviations listed in the table were calculated using replicate samples.

Table 1: Summary of leaching results relative to amount of sediment leached.

Sediment	Fraction	pH	Mass Element per Mass Sediment (µg/g, x10^5)					
			Be	Ni	Cd	Ba	Pb	U
Site E-F	Pan	6.8	6.9	190	7.8	10,000	92	299
		4.9	3.3	290	14	8100	-1200	274
	Mid.	6.8	3.1	170	3.3	7500	110	270
		4.9	1.1	200	-4.6	7800	-1500	270
	Undiff.	6.8	4.7	210	-2.4	7900	-76	328
		4.9	2.9	227	-3.9	7800	-150	280
Skunk Works	Undiff.	6.8	2.8	37	-1.29	2500	18	100
		4.9	2.4	41	-5.5	2800	-82	93
Standard Deviation			13	34	30	300	26	50

At the extremely low concentrations measured in the leachate solutions, the comparison of data to a detection limit, as well as to a standard deviation based on replicate samples, is important. Method blanks were analyzed by ICP-MS, and the mean and standard deviation of these blanks were calculated for each element; five times this standard deviation will be used as a detection limit. These detection limits, as well as uncorrected concentration results are collected in Table 2.

Results of analysis of beryllium, cadmium and lead in leachate solutions are ambiguous. Beryllium is just detectable in most cases; the standard deviation of replicate samples listed Table 1, however, is larger than any of the Be values in Table 1. When analytical and methodological uncertainties are taken into account, then, beryllium is effectively below the level of quantitation. With respect to detection limit comparisons, cadmium is similar to beryllium, though cadmium is below detection limits for Skunk Works sediment. Lead is clearly not easily analyzed by ICP-MS, as exemplified by the large negative results seen for over half of the samples. These observations indicate that little is to be gained by further analysis of Be, Cd, and Pb results. In the cases of Be and Cd, neither is quantifiable because only minuscule amounts leached from the sediments during experiments.

Nickel, barium and uranium leached from both sediments in great enough quantity to provide analytical results well above detection limits, and calculated values greater than standard deviations based on replicate samples. Emphasis will be placed on these results, not only since they are statistically significant, but also because the concentrations listed in Table 1 indicate that leaching is likely to be a much more significant mode of transport for them than for Be and Cd, and possibly for Pb.

Effect of Sediment Sampling Site on Leaching

Twenty-four hour leaching experiment results from Table 1 show that greater concentrations of Ni, Ba, and U were leached from site E-F sediment than from Skunk Works sediment. Preliminary sediment digestate analyses by ICP-AES indicate that site E-F bulk sediment contains higher concentrations of all elements tested (though some of these analyses gave results below calculated detection limits). This is likely the source of most of the disparity in concentration of leached elements. Differences in surface properties of the sediments may also contribute to differences in leached concentrations; extent of this effect, however, is inaccessible from these data.

Effect of pH on Leaching

Only two leaching-solution pH values were investigated in these experiments. For the three metals for which results were quantifiable, concentration of leached metal never varied by as much as a factor of two in a system where pH was the only variable. The

Table 2: Uncorrected ICP-MS concentration values and calculated detection limits.

Sediment	Fraction	pH	Concentration, or Detection Limit (µg/L)					
			Be	Ni	Cd	Ba	Pb	U
Site E-F	Pan	6.8	0.025	1.118	0.075	49.75	0.802	1.478
		4.9	0.011	1.557	0.103	38.96	1.219	1.308
	Mid.	6.8	0.007	1.023	0.053	37.58	0.916	1.381
		4.9	0.000	1.128	0.014	37.13	0.153	1.255
	Undiff.	6.8	0.027	1.227	0.024	38.57	0.179	1.604
		4.9	0.018	1.344	0.035	38.65	0.090	1.413
Skunk Works	Undiff.	6.8	0.018	0.405	0.030	12.72	0.637	0.514
		4.9	0.016	0.415	0.027	13.96	0.419	0.459
Detection Limit			0.009	0.207	0.048	0.25	1.137	0.013

effect of pH on leaching of U and Ba cannot be determined from these results. Nickel was uniformly (though only slightly) leached to a greater extent by soil at pH 4.9 than by soil at pH 6.8. Over the range studied, pH is not a strongly important variable in leaching of the elements quantified here.

Effect of Sediment Size on Leaching

The mass ratios of different size fractions relative to one another varied notably between site E-F and Skunk Works sediment. Fifteen percent of a sample of site E-F sediment passed through a #200 sieve, while 65 percent passed through a #10 sieve but was retained on a #200 sieve. The remainder (20 percent) was retained on a #10 sieve. Two percent of a sample of Skunk works sediment passed through a #200 sieve, while 96 percent was between #200 and #10 and two percent was retained on a #10 sieve.

Smaller particles have greater surface-area-to-mass ratios than larger particles; this greater area for leaching is likely to enhance leaching in smaller particles. Comparison of the pan fraction to the fraction between sieve sizes 200 and 10 bears out this trend for Ni, Ba and U (see Table 1). Ignoring quantitation problems for a moment, one sees that the same is true for Be and Cd. As with pH, however, sediment size does not have a dramatic effect on extent of leaching of any of these metals.

Effect of Time on Leaching

In each of the elements quantifiable by these tests, time had a marked impact on mass of element leached per unit mass sediment. Figures 1 through 8 show leachate concentrations with time for both site E-F and Skunk Works sediments for the elements Be, Ni, Ba, and U. Error bars are based on standard deviations of replicates run on a subset of samples; they are placed one standard deviation value above and below the calculated concentration. Analysis results of kinetics experiments for Be, Pb and Cd were not statistically significant. Error bars in Figures 1 and 2, results of experiments on Be, are representative of the inconclusive nature of kinetics results for these three elements.

Nickel concentration in site E-F leachate increased at each sampling time through the 72-hour sampling. After this point, Ni concentration appears to have decreased slightly, though within standard error this apparent decrease could be interpreted as an equilibrium state with respect to Ni leaching. It is possible, however, that concentration of Ni in solution did decrease slightly. Nickel may have sorbed to the container at a slow rate, or water chemistry changes occurring during the experiment may have changed the form of Ni in solution to a more readily sorbed complex. Concentration of Ni leached from Skunk Works sediment reached equilibrium much more quickly than that leached from site E-F sediment. This is likely a result of the fact that equilibrium concentration of Ni leached from Skunk Works sediment is less than half of that leached from site E-F sediment.

Figure 1: Site E–F, Beryllium Leaching With Time

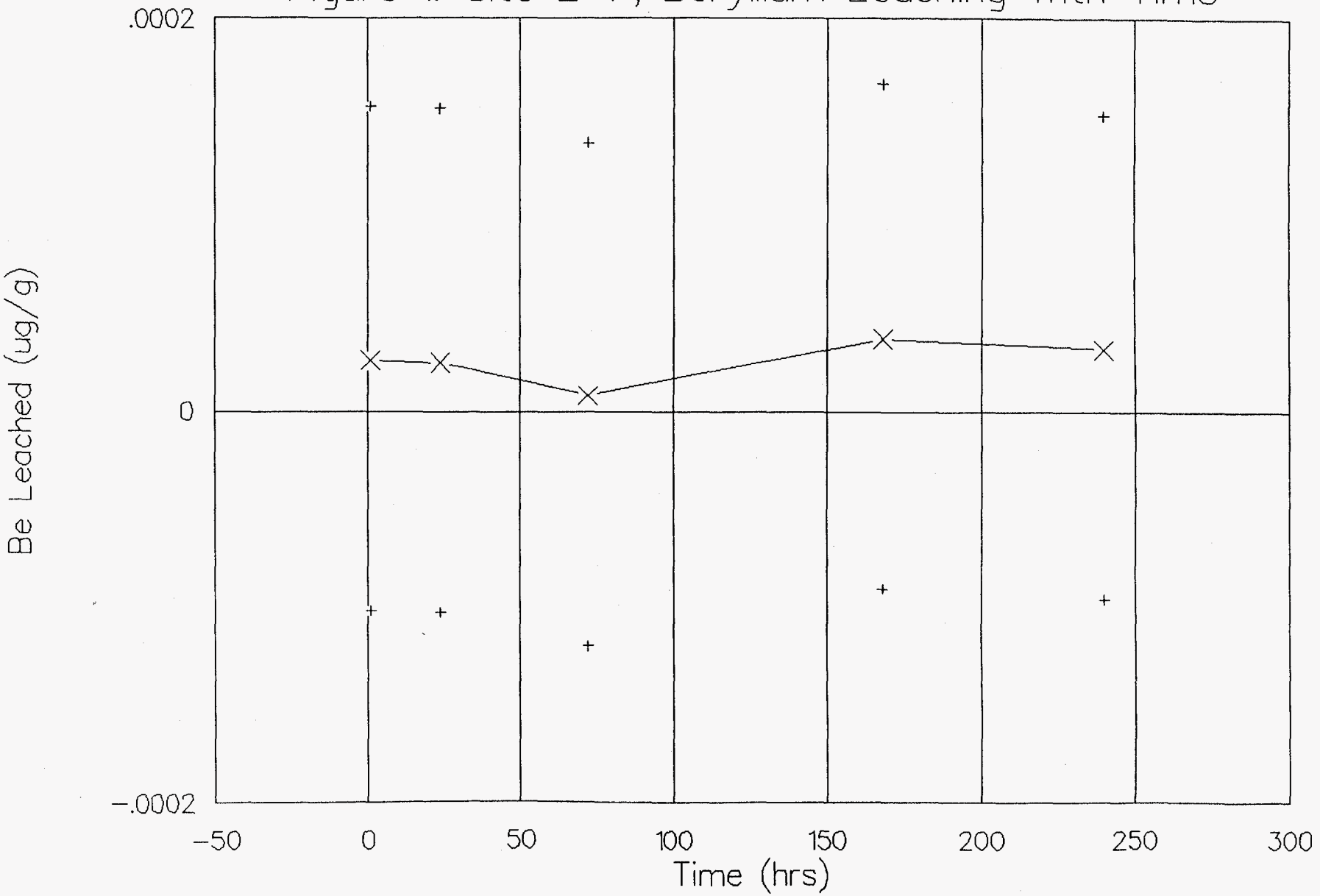

Figure 2: Skunk Works, Beryllium Leaching With Time

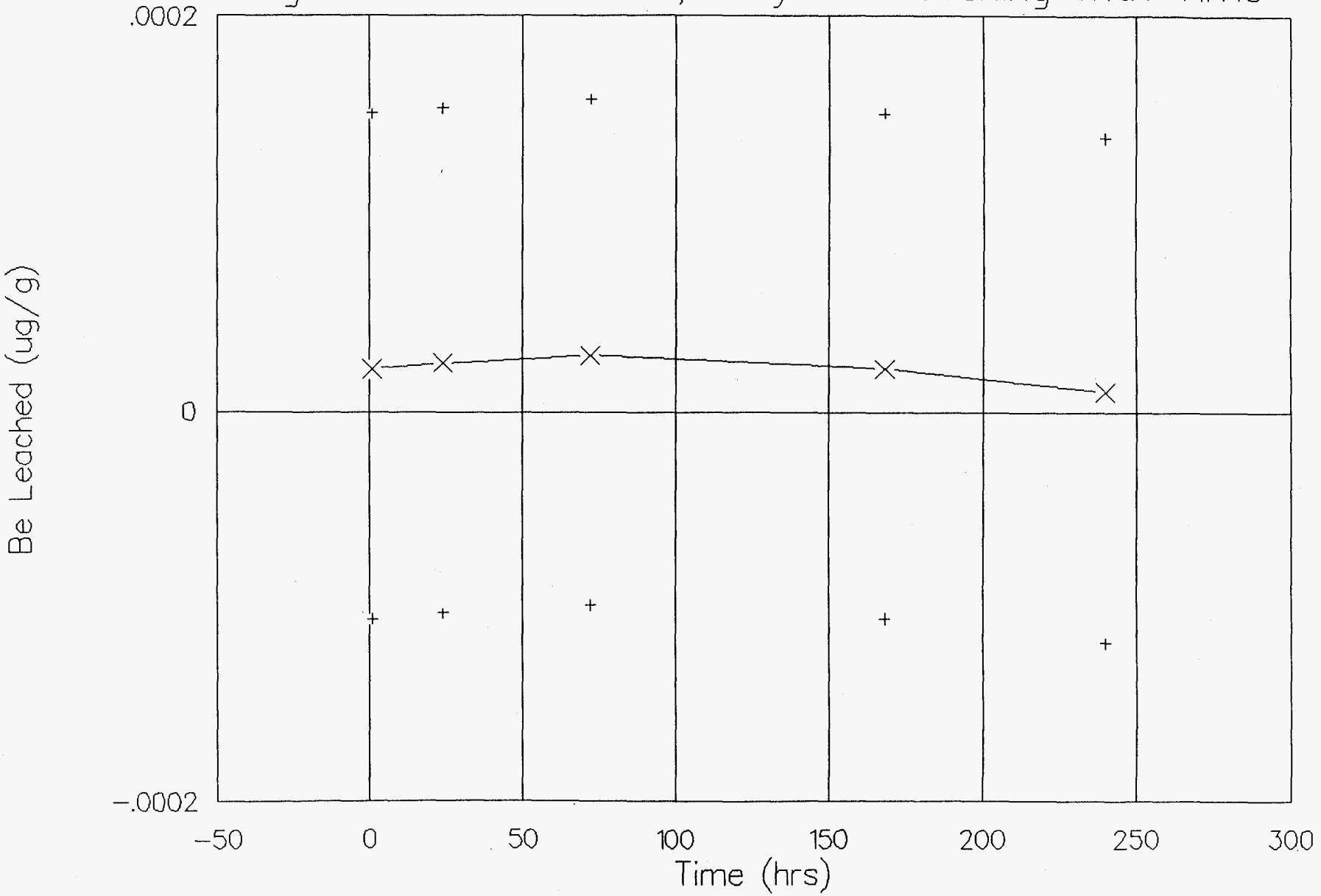

Figure 3: Site E–F, Nickel Leaching With Time

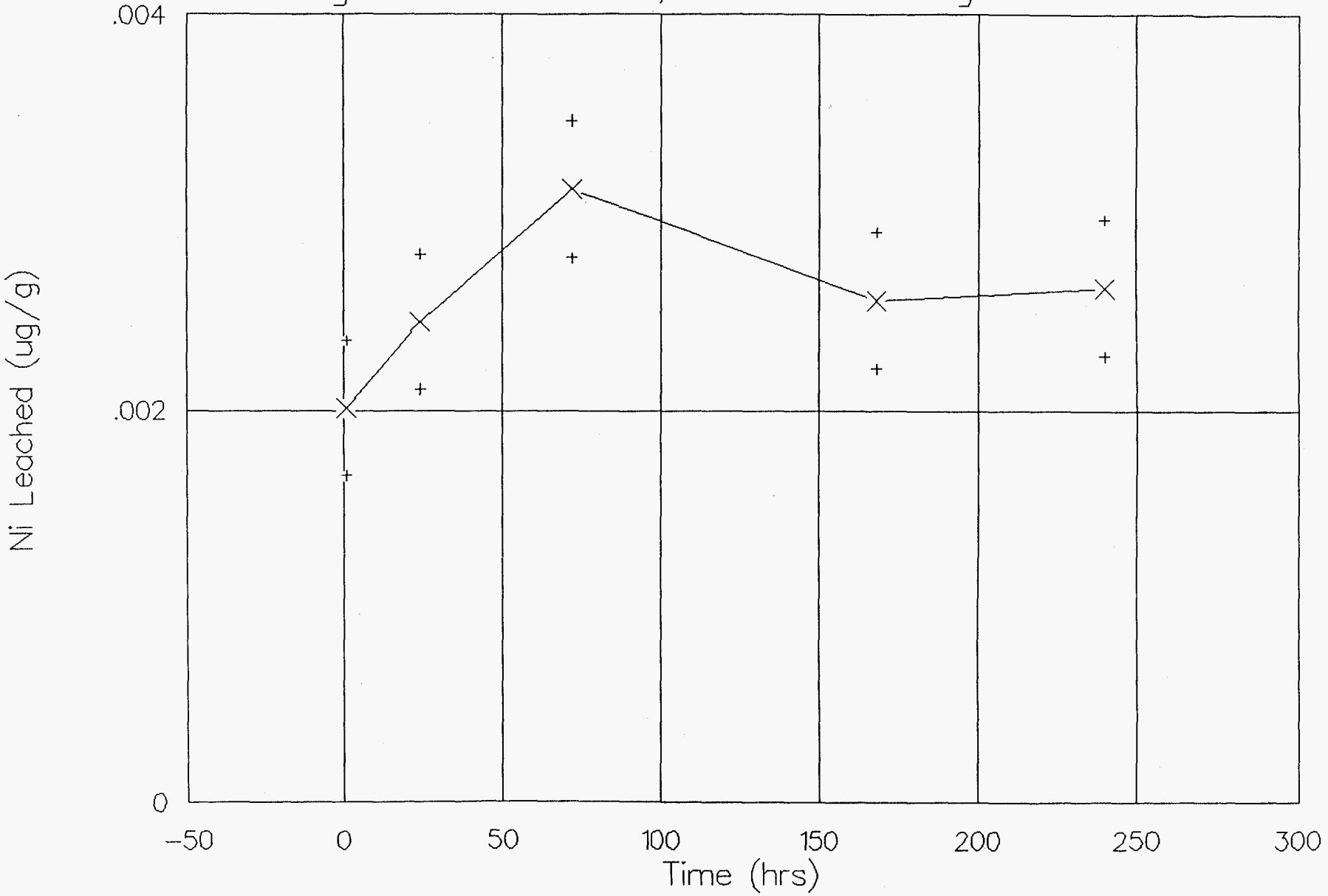

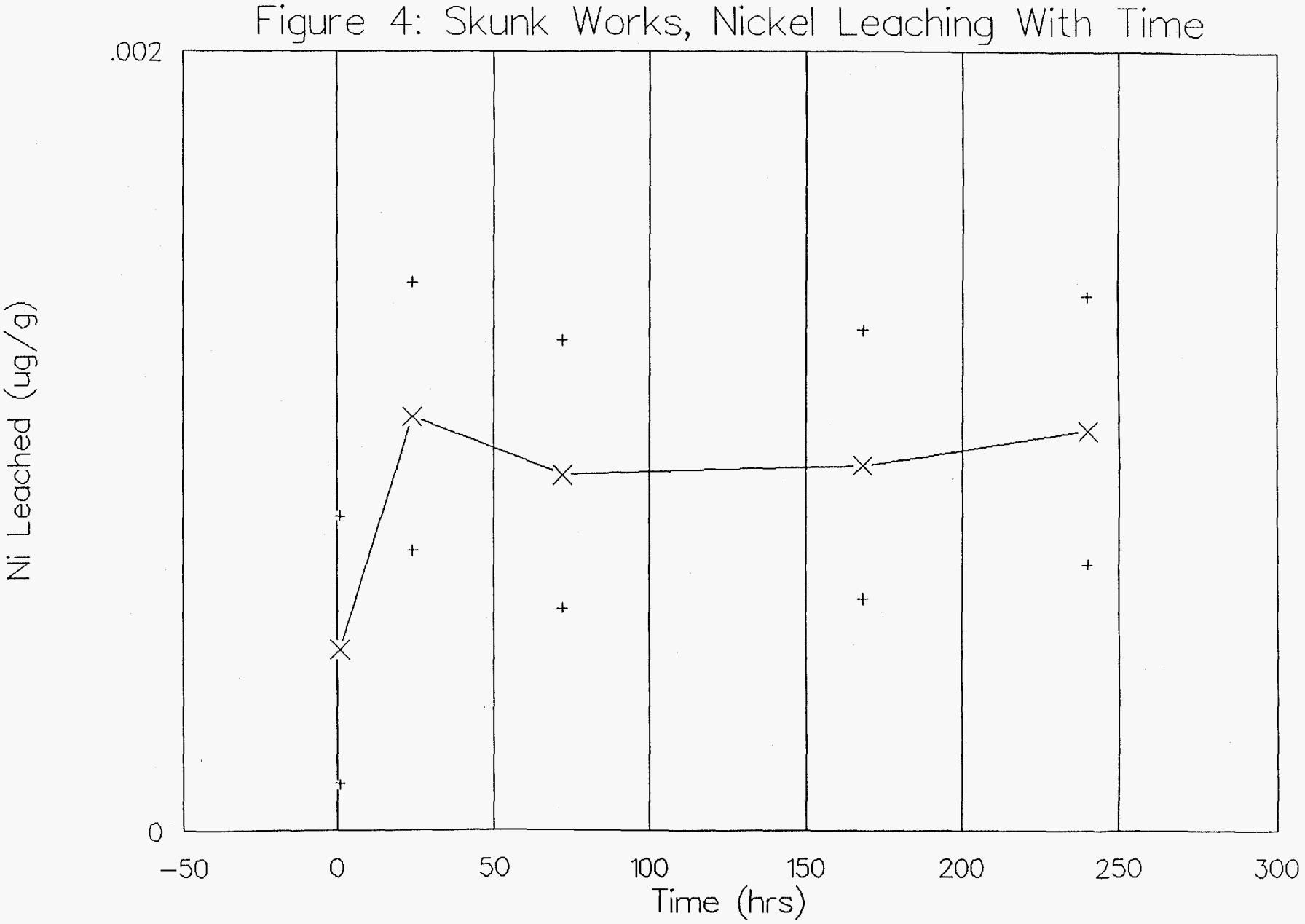
Figure 4: Skunk Works, Nickel Leaching With Time
.002
0
Ni Leached (ug/g)
-50
0
50
100
150
200
250
300
Time (hrs)

Figure 5: Site E–F, Barium Leaching With Time

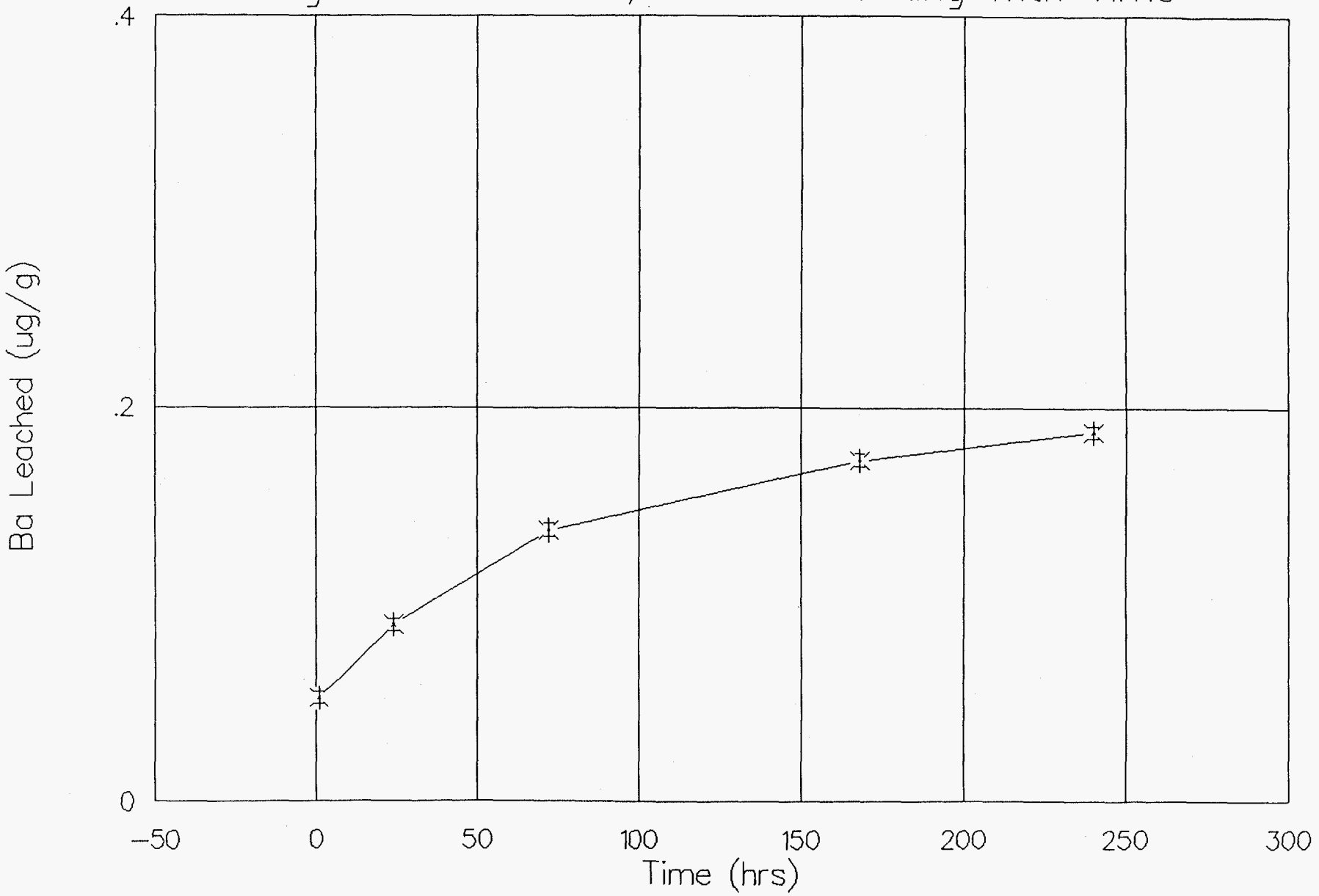

Figure 6: Skunk Works, Barium Leaching With Time

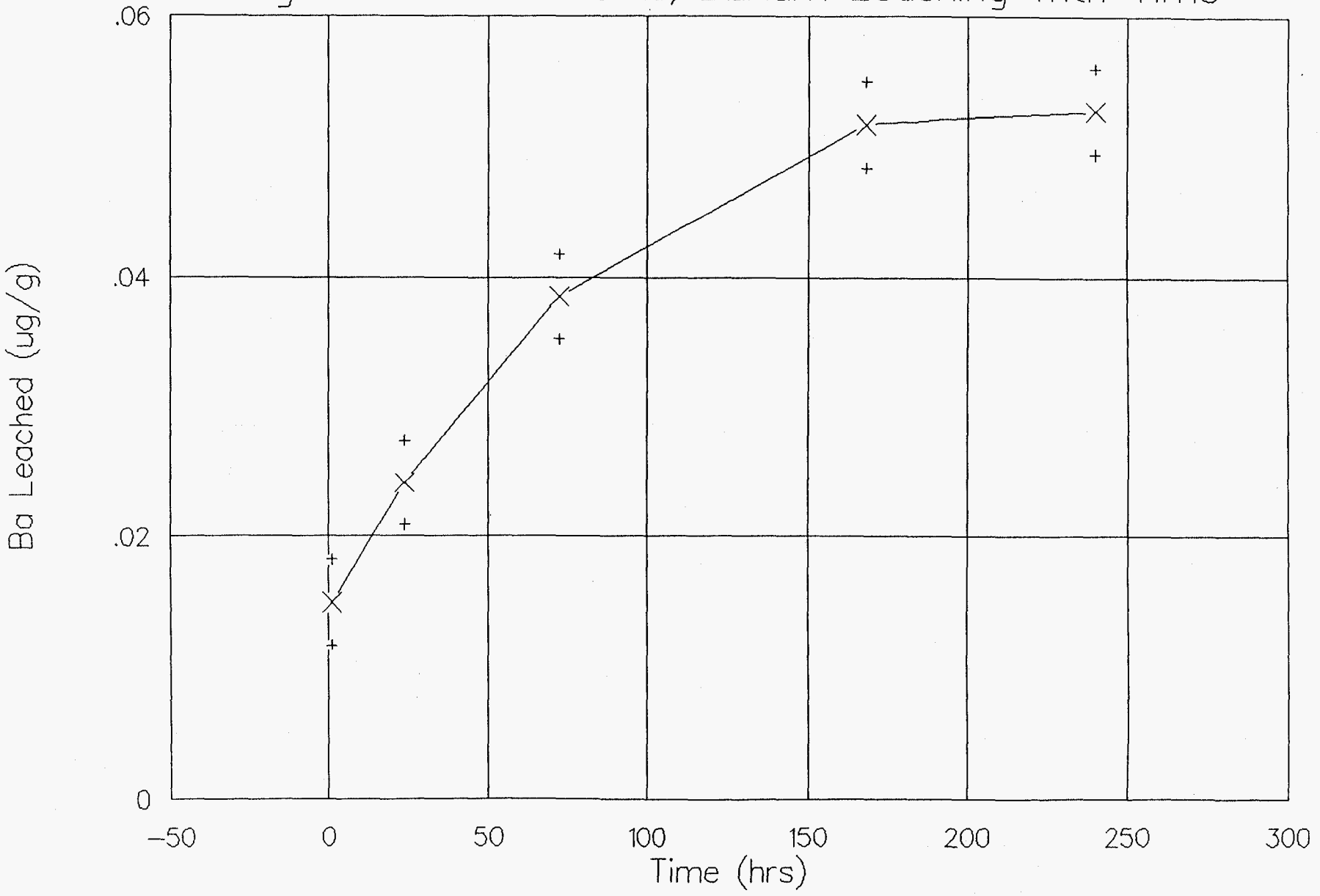

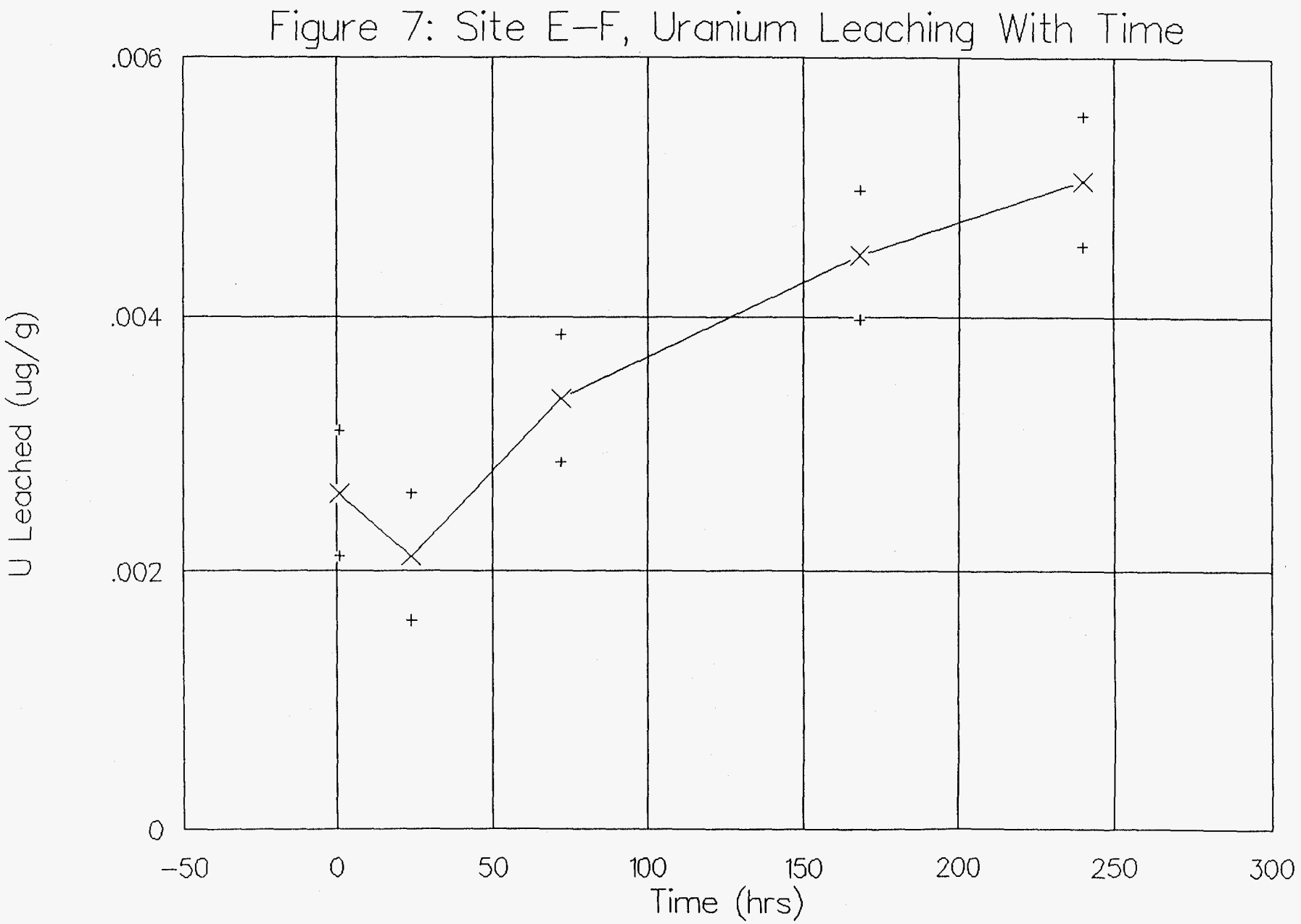
Figure 7: Site E–F, Uranium Leaching With Time
.006
.004
.002
0
U Leached (ug/g)
–50
0
50
100
150
200
250
300
Time (hrs)

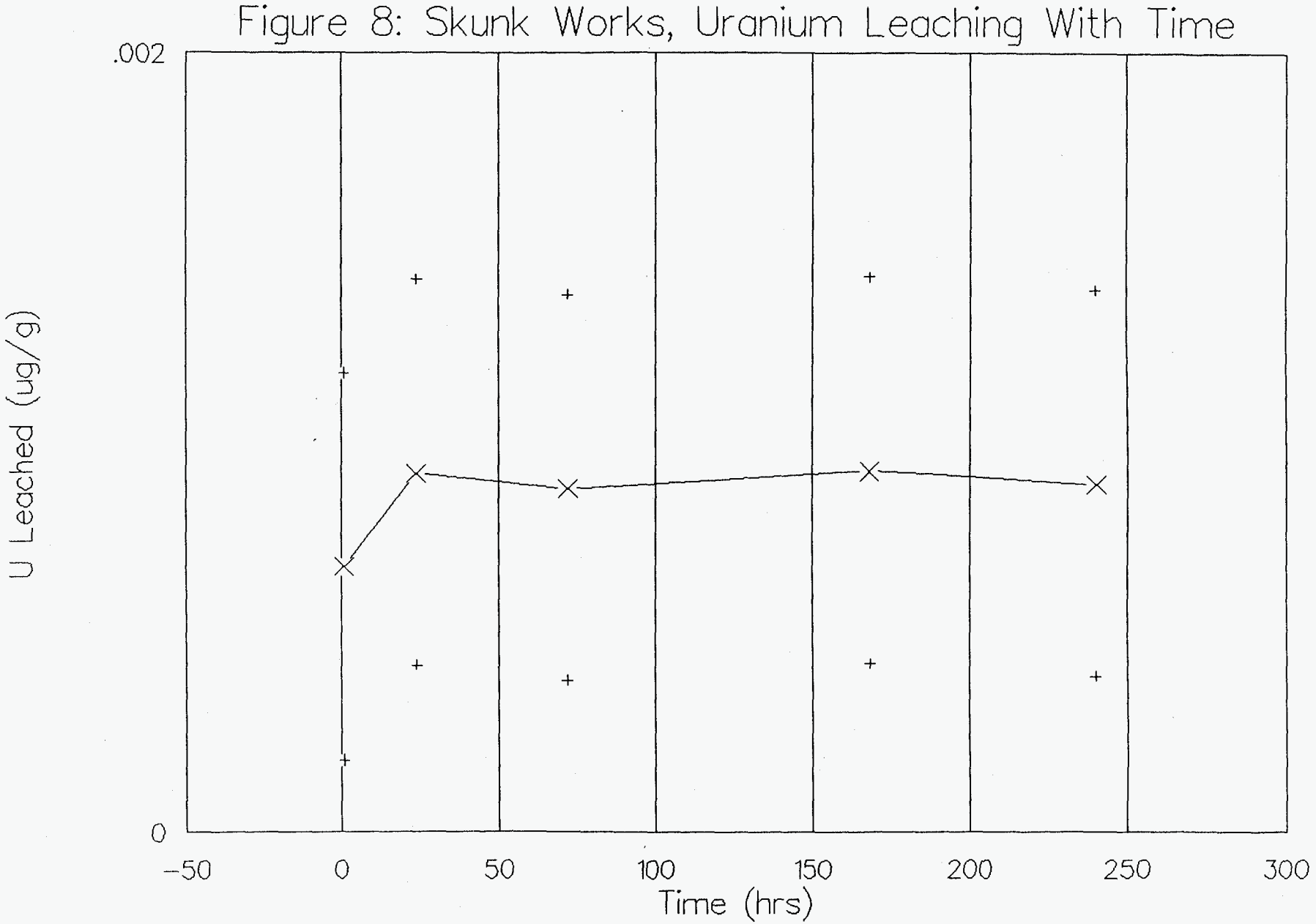
Figure 8: Skunk Works, Uranium Leaching With Time
.002
0
U Leached (ug/g)
-50
0
50
100
150
200
250
300
Time (hrs)

Concentrations of Ba leached from site E-F and from Skunk Works sediments behaved in a very similar fashion with time, though absolute concentrations at a given time were a factor of 5 to 10 higher in site E-F leachates. Concentrations from both sediment types increased quickly at first and then more slowly as they approached the 10-day mark. Concentrations in both increased approximately 3.5 times from the 1-hour sampling to the 10-day sampling.

Behavior of uranium leaching with time was similar to that of Ni in both form and concentration. Site E-F sediments produced a statistically significant increase in leachate concentration with time. Between 1 and 24 hours, however, a re-sorption event seemed to occur, which could be a result of any of the effects mentioned with respect to Ni. Concentrations of U leached from Skunk Works sediments showed slight increase over the first 24 hours, but this increase is not significant within plus or minus 1 standard deviation.

Sediment Digestion

In an effort to compare concentration of elements leached to concentration of these elements in the sediment matrix, samples of the sediment were digested, and the digestates analyzed using ICP-AES. The pan fractions and mid fractions of both site E-F and Skunk Works sediments were digested and analyzed; the sediment retained on the #10 sieve was too large to be digested efficiently. The results of these analyses and mass element per mass sediment values calculated from them are collected in Table 3.

A detection limit was calculated for each element. This detection limit is 5 times the standard deviation of method blanks. This calculation produces a fairly high estimate of detection limit, since the method blank includes uncertainty not only in analysis, but also in the entire digestion process. Based on these detection limits, Be and Ba are easily detectable, and Ni results are close to the detection limit. Lead results are also near detection limits, with the exception of the negative result for the Skunk Works mid fraction. ICP-AES results for Cd are clearly too low to be quantifiable, and U is not analyzable by ICP-AES at these concentrations.

The mass-per-mass values in Table 3 can be used to calculate a concentration of element in the bulk sediment by adding together the products of the concentration of each size fraction and the percent mass contributed to the bulk soil by each size fraction. Inherent in this technique is the assumption that the contribution of the #10 sieve retentate would be negligible. Once a concentration of the element in bulk sediment is available, it can be compared to average mass-per-mass leachate values from Table 1 to determine a fraction of total element leached. For this purpose, undifferentiated sediment results from Table 1 were used (i.e., the contribution to leached concentration of sediment retained on a #10 sieve was assumed to be negligible). Only Be, Ni and Ba gave statistically significant results in both leaching and digestion tests; fractions leached of these three elements are compiled in Table 4. The fractions of Ni and Ba leached in 24 hours are similar to one another, and are approximately 10 times higher than the

Table 3: Results of ICP-AES Analyses of Digested Sediments.

		Be	Ni	Cd	Ba	Pb	U
E-F, Pan Fraction	Digestate Concentration, µg/L	6.6	38	2.1	1600	100	-300
	Mass Element per Mass Sediment, µg/g	1.9	8.2	0.86	460	13	37
E-F, Mid Fraction	Digestate Concentration, µg/L	6	36	-0.2	840	66	-670
	Mass Element per Mass Sediment, µg/g	1.8	7.8	0.21	240	3.2	-68
Skunk Works, Pan Fraction	Digestate Concentration, µg/L	5.6	24	-0.1	1100	63	-1100
	Mass Element per Mass Sediment, µg/g	1.7	4.6	0.25	320	2.2	-220
Skunk Works, Mid Fraction	Digestate Concentration, µg/L	3.6	15	-1.5	206	-5.5	-880
	Mass Element per Mass Sediment, µg/g	1.1	1.7	-0.16	58.6	-17.4	-130
Detection Limit, µg/L		0.22	41	3.7	4.1	69	590

Table 4: Fraction of Elements Leached from Sediments

Sediment	Be	Ni	Ba
Site E-F	2.7×10^{-5}	3.5×10^{-4}	3.5×10^{-4}
Skunk Works	2.4×10^{-5}	2.3×10^{-4}	4.2×10^{-4}

amount of Be leached. In addition, for any given element of the three, the fraction leached from site E-F and Skunk Works sediments are very similar to one another, indicating that the sediments have similar leaching properties.

Conclusions, Recommendations for Future Work

All of the variables tested for their effect upon leaching characteristics -- pH, sediment size, sediment location, and leaching time -- had detectable effects for at least some of the elements tested. For elements for which reliable analyses were available, however, none of these parameters modified leached concentrations by as much as a factor of ten over the range tested (though the difference between concentration of Ni leached from site E-F and from Skunk Works sediments approached this level). Experiments on pH differences and size fraction differences provided particularly unremarkable results.

Based on this relative lack of susceptibility to changes in the variables tested, the most noteworthy results of these experiments are the actual concentrations of the elements of interest leached from the sediments. Barium was leached in the greatest concentrations from the sediments, averaging nearly 0.1 μg/g leached from site E-F sediments and nearly 0.03 μg/g leached from Skunk Works sediments. Both Ni and U varied between 1 and 5 ng/g leached from site E-F sediments and 0.3 and 1 ng/g leached from Skunk Works sediments. The levels of the remaining elements were generally below the standard deviations in their measurements, which were in the hundreds of picograms per gram.

Based on these tests, it is suggested that sampling of runoff water from actual storm events on the Los Alamos National Laboratory site would comprise by far the most useful follow-up experiments. Though care has been taken in these laboratory experiments to mimic rainwater and runoff water conditions, there is no better way to estimate the effects of stormwater leaching than to measure it directly. Removal, transport and storage of sediment samples creates unavoidable changes in particle surface chemistry and in speciation of elements associated with these surfaces. Though this laboratory study is a good general look at the extent to which these metals are leached, analysis of runoff captured, filtered and acid-preserved in the field would be an excellent test of the validity of these results. If such field sampling is undertaken, it is in addition highly recommended that "trace-metal clean" sampling and analysis techniques be used throughout the process.

If more laboratory experiments are considered desirable, the effects of organic and inorganic colloids and of dissolved and particulate organic carbon are likely to be significant. It may also be desirable to find techniques capable of measuring trace quantities of the elements which ICP-MS and ICP-AES were not capable of detecting (i.e., it may be desirable to find an ICP-MS capable of analyzing digestates which contain hydrofluoric acid to obtain an accurate value of uranium in sediments).

sample	sediment	pH	fraction	LANL Sediment Leaching Results Effect of pH Mass element/Mass soil (ug/g) Be	Ni	Cd	Ba	Pb	U
3F	E-F	SOIL	PAN	6.904e-5	1.938e-3	7.757e-5	1.008e-1	9.164e-4	2.999e-3
4F	E-F	RAIN	PAN	3.352e-5	2.929e-3	1.408e-4	8.145e-2	-1.29e-2	2.739e-3
5F	E-F	SOIL	MID	3.147e-5	1.712e-3	3.307e-5	7.462e-2	1.126e-3	2.749e-3
6F	E-F	RAIN	MID	1.078e-5	2.047e-3	-4.63e-5	7.827e-2	-1.53e-2	2.650e-3
L1	E-F	SOIL	UNDIFF	4.704e-5	2.064e-3	-2.38e-5	7.901e-2	-7.58e-4	3.283e-3
L2	E-F	RAIN	UNDIFF	2.940e-5	2.277e-3	-3.91e-5	7.776e-2	-1.48e-3	2.843e-3
L3	SW	SOIL	UNDIFF	2.810e-5	3.683e-4	-1.29e-5	2.550e-2	1.797e-4	1.027e-3
L4	SW	RAIN	UNDIFF	2.435e-5	4.092e-4	-5.48e-5	2.826e-2	-8.22e-4	9.301e-4

Net concentrations in leachate samples, pH/size fraction experiments, micrograms per liter

				Be	Ni	Cd	Ba	Pb	U
3F	E-F	SOIL	PAN	.0340	.9544	.0382	49.6310	.4513	1.4771
4F	E-F	RAIN	PAN	.0160	1.3980	.0672	38.8773	-6.1660	1.3073
5F	E-F	SOIL	MID	.0158	.8594	.0166	37.4610	.5655	1.3801
6F	E-F	RAIN	MID	.0051	.9690	-.0219	37.0473	-7.2315	1.2543
L1	E-F	SOIL	UNDIFF	.0229	1.0047	-.0116	38.4624	-.3689	1.5983
L2	E-F	RAIN	UNDIFF	.0146	1.1307	-.0194	38.6161	-.7343	1.4120
L3	SW	SOIL	UNDIFF	.0139	.1822	-.0064	12.6124	.0889	.5080
L4	SW	RAIN	UNDIFF	.0120	.2017	-.0270	13.9261	-.4052	.4584

Effect of Kinetics

sediment	time (hrs)	sample	Be (ug/g)	Ni (ug/g)	Cd (ug/g)	Ba (ug/g)	Pb (ug/g)	U (ug/g)
E-F	1.0000	L7	2.643e-5	2.012e-3	9.409391e-6	5.159709e-2	5.504349e-1	2.617212e-3
E-F	24.0000	L10	2.523e-5	2.452e-3	-2.12212e-5	8.895718e-2	-7.69968e-4	2.118915e-3
E-F	72.0000	L13	8.408e-6	3.120e-3	-5.02501e-5	1.369136e-1	-1.30190e-3	3.366560e-3
E-F	168.0000	L16	3.784e-5	2.560e-3	8.608591e-6	1.728223e-1	-1.71872e-3	4.482874e-3
E-F	240.0000	L19	3.243e-5	2.624e-3	1.657654e-4	1.874673e-1	4.662653e-4	5.056246e-3
SW	1.0000	L8	2.223e-5	4.643e-4	3.52528e-5	1.491594e-2	9.05356e-5	6.85026e-4
SW	24.0000	L11	2.504e-5	1.064e-3	5.8087e-6	2.418462e-2	-3.50725e-4	9.275893e-4
SW	72.0000	L14	2.924e-5	9.146e-4	2.22333e-5	3.855475e-2	-4.88732e-5	8.885308e-4
SW	168.0000	L17	2.243e-5	9.394e-4	-2.86429e-5	5.176733e-2	-1.13190e-3	9.335983e-4
SW	240.0000	L20	1.042e-5	1.029e-3	-1.94291e-5	5.281931e-2	-3.13269e-4	9.007491e-4

Method Std Deviations

	Be (ug/L)	Ni (ug/L)	Cd (ug/L)	Ba (ug/L)	Pb (ug/L)	U (ug/L)
Avg	-.0013	.1	.0	.1	.6	.0032
Std Dev	.0019	.0	.0	.1	.2	.0027

Net concentrations in leachate samples, kinetics experiments, micrograms per liter								
sample	sediment	time (hrs)	Be	Ni	Cd	Ba	Pb	
L7	E-F	1.0	.0132	1.0048	.0047	25.7728	274.9428	1.3073
L10	E-F	24.0	.0126	1.2249	-.0106	44.4342	-.3846	1.0584
L13	E-F	72.0	.0042	1.5582	-.0251	68.3885	-.6503	1.6816
L16	E-F	168.0	.0189	1.2788	.0043	86.3249	-.8585	2.2392
L19	E-F	240.0	.0162	1.3105	.0828	93.6401	.2329	2.5256
L8	SW	1.0	.0111	.2318	.0176	7.4468	.0452	.3420
L11	SW	24.0	.0125	.5310	.0029	12.0742	-.1751	.4631
L14	SW	72.0	.0146	.4566	.0111	19.2485	-.0244	.4436
L17	SW	168.0	.0112	.4690	-.0143	25.8449	-.5651	.4661
L20	SW	240.0	.0052	.5136	-.0097	26.3701	-.1564	.4497

Samples Generated
Los Alamos National Laboratories
Sediment Leaching Project

Russ Herrin

1F Soil pH control corresponding to 3F through 6F

2F Rainwater pH control corresponding to 3F through 6F

3F 29.583 g site E-F pan fraction sediment and 60.072 g soil pH Milli-Q

4F 29.159 g site E-F pan fraction sediment and 61.092 g rainwater pH Milli-Q

5F 30.550 g site E-F #200<x<#10 sediment and 60.856 g soil pH Milli-Q

6F 29.712 g site E-F #200<x<#10 sediment and 62.776 g rainwater pH Milli-Q

L1 30.074 g undifferentiated E-F sediment and 61.776 g soil pH Milli-Q

L2 30.015 g undifferentiated E-F sediment and 60.443 g rainwater pH Milli-Q

L3 30.014 g undifferentiated Skunk Works sediment and 60.673 g soil pH Milli-Q

L4 30.251 g undifferentiated Skunk Works sediment and 61.377 g rainwater pH Milli-Q

L5 Soil pH control corresponding to L1 through L4

L6 Rainwater pH control corresponding to L1 through L4

Samples L7 through L21 correspond to a kinetics experiment using slurries and controls in bottles K1, K2 and K3. The contents of these bottles are described first.

K1 200.2 g undifferentiated E-F sediment and 400.8 g soil pH Milli-Q

K2 200.0 g undifferentiated Skunk Works sediment and 400.6 g soil pH Milli-Q

K3 Soil pH control corresponding to K1 and K2

Samples:

L7 1-hour sampling of K1

L8 1-hour sampling of K2

L9 1-hour sampling of K3

L10 1-day sampling of K1

L11 1-day sampling of K2

L12 1-day sampling of K3

L13 3-day sampling of K1

L14 3-day sampling of K2

L15 3-day sampling of K3

L16 7-day sampling of K1

L17 7-day sampling of K2

L18 7-day sampling of K3

L19 10-day sampling of K1

L20 10-day sampling of K2

L21 10-day sampling of K3

L22 Milli-Q

L23 L18 duplicate

L24 Milli-Q

L25 4F duplicate

L26 L2 duplicate

Sediment Digestions

D1 0.184 g E-F pan fraction sediment digestate

D2 0.193 g Skunk works pan fraction sediment digestate

D3 0.189 g E-F #200<x<#10 fraction sediment digestate

D4 0.187 g Skunk Works #200<x<#10 fraction sediment digestate

D5 Method/reagent blank

D6 Method/reagent blank

D7 0.204 g leached E-F sediment, <#200 mesh (soil pH)

D8 0.211 g leached E-F sediment, <#200 mesh (rain pH)

D9 Method/reagent blank

D10 Method/reagent blank

D11 0.224 g leached E-F sediment, 10>x200 mesh (soil pH)

D12 0.210 g leached E-F sediment, 10>x>200 mesh (rain pH)

Report on the
Runoff, Sediment, and Contaminant Transport Research
at
Big Buck Canyon,
Los Alamos National Laboratory

for

Naomi M. Becker, Ph.D.
Group EES-3
Los Alamos National Laboratory
New Mexico

by

David C. Perry
and
Professor John A. Hoopes
Department of Civil and Environmental Engineering
University of Wisconsin, Madison

2 June 1995

TABLE OF CONTENTS

Executive Summary

Research on the runoff, sediment, and contaminant transport in Big Buck Canyon at the Los Alamos National Laboratory began in 1993. The final research goal is to estimate how fast and how much contaminated sediment is moving in the canyon. Due to equation of state experiments involving high explosives, soils in the vicinity of the three test sites have been contaminated with heavy metals such as uranium and cadmium. There are three main parts to the research that will eventually be combined to address the final goal of estimating total contaminant movement. The first part involves the collection and interpretation of experimental field data, such as rainfall and runoff amounts. The second part involves numerical modeling the watershed response to rainfall inputs. The third part involves experimental chemistry work to evaluated the concentration of contaminants in a representative sample of sediment.

Monitoring stations have been installed to measure precipitation, streamflow, and suspended sediment concentration. These measurements will assist in understanding the hydrologic processes at work in the watershed to transport materials. The measurements will also be used to calibrate the numerical simulation model. The value of a numerical model to simulate the rainfall/runoff process is two-fold. First, the model can be used to test the sensitivity of the response to changes in input values. A sensitivity study of this sort will identify the most important and least important input parameters. Additional research work can then be focused on the important matters while avoiding additional work on unimportant matters. Second, the model can be used to reconstruct a simulated record of flow for the past fifty years; the time period that the Laboratory has used Big Buck Canyon for explosives testing. To estimate the movement of contaminants over this period, a record of flow is needed. On-site flow measurement began with this project in 1993; thus, the existing record of flow is too short. Fortunately, precipitation records are available for the entire period. Using the model with the long precipitation record, a simulated record of flow can be reconstructed. The final integration of the existing experimental chemistry work with the simulation of runoff and sediment movement remains to be defined.

The details about the model development and testing are presented. The simulation of a large flood in 1991 did not compare well with observations of the event. The model seriously underpredicted the flow out of the watershed because the value of the hydraulic conductivity in the channel was too large. The infiltration of water into the channel bed, known as transmission losses, is a direct function of hydraulic conductivity. Field measurements of hydraulic conductivity yielded values that are much larger than those found in the literature. Consequently, the high input values of hydraulic conductivity produced model results that underestimated the flow. Future research on the process of transmission losses is recommended to resolve this issue and improve the accuracy of the model results.

This report summarized the research progress over the past two years and should be useful to those who will continue the investigation of contaminant movement in the watershed. The contents of the report are intended to explain the choices and developments that have lead the research to the present state. Attached are a number of appendices that provided detailed information on individual project tasks such as the soil sample analysis or the KINEMAT program input files.

models for arid conditions. Therefore, this research integrates field measurements with numerical modeling and contaminant chemistry with the goal of predicting the movement of heavy metals in this arid watershed.

1.2 Background

Since 1985, Naomi Becker has studied the influence of hydraulic and geomorphologic factors on the transport of depleted uranium in Potrillo Canyon, another watershed at the Laboratory which is in the same vicinity as Big Buck Canyon. Both Potrillo and Big Buck canyons are characterized by similar physical features and contaminant inputs.

This research is an expansion of Dr. Becker's work which incorporates some of the same techniques, as well as some new techniques, to asses the hydrologic response to the watershed. The sediment sampling techniques developed for Potrillo Canyon have been applied to Big Buck Canyon. Likewise, the precipitation measurement system is the same. The streamflow measurement system, however, is new. Since installation the system has not yet experienced a runoff event to test its performance. The application of a numerical model to Big Buck Canyon to simulate the rainfall, runoff, and erosion processes is also new.

Figure 1 shows a layout of the Laboratory which identifies the technical areas by number. Big Buck Canyon is associated with TA-39 and Potrillo Canyon is associated with TA-36. State Road 4 marks the downstream end of both watersheds studied.

1.3 Watershed Description: Big Buck Canyon

Big Buck canyon is a narrow semi-arid watershed that is incised into a mesa formation. The narrow mesa tops and steep canyon walls bound the canyon on both sides. The watershed drains to an outlet culvert under State Road 4 (called Culvert 1). After the culvert the stream continues a short distance to its confluence with the Ancho Canyon channel. The drainage area above Culvert 1 is 5.54 km^2.

The watershed can be broken up into two parts, a lower watershed and an upper watershed, as shown in Figure 2. The lower watershed contains the access road leading up to the test sites in Technical Area 39 (TA-39) and is characterized in cross section by mesa tops, canyon walls, an alluvial valley floor, and a sandy channel. The channel slope in the lower watershed averages 1.8% overall, ranging locally from 1.5% to 2.5%.

The upper watershed is much steeper and can only be accessed on foot. The upper watershed cross sections do not have a valley floor; instead, the canyon walls drain directly into the steep stream channels. Typical channel slopes in the upper watershed range from 3% to 14%. The upper watershed is about half of the total watershed area.

The main channel extends from the mesa associated with TA-49 and continues through the upper watershed to Firing Site 8 in TA-39. It then joins with a small tributary from Firing Site 7 and continues through the lower watershed to State Road 4. In the upper watershed, one tributary joins the main channel about half way between TA-49 and Firing Site 8. I will call this tributary the "saddle" tributary since it leads up to a saddle back formation between Big Buck Canyon and the neighboring Water Canyon. In the lower watershed, one tributary joins the main channel at Culvert 12 after flowing past Firing Site 6. This tributary watershed is also steep and narrow like

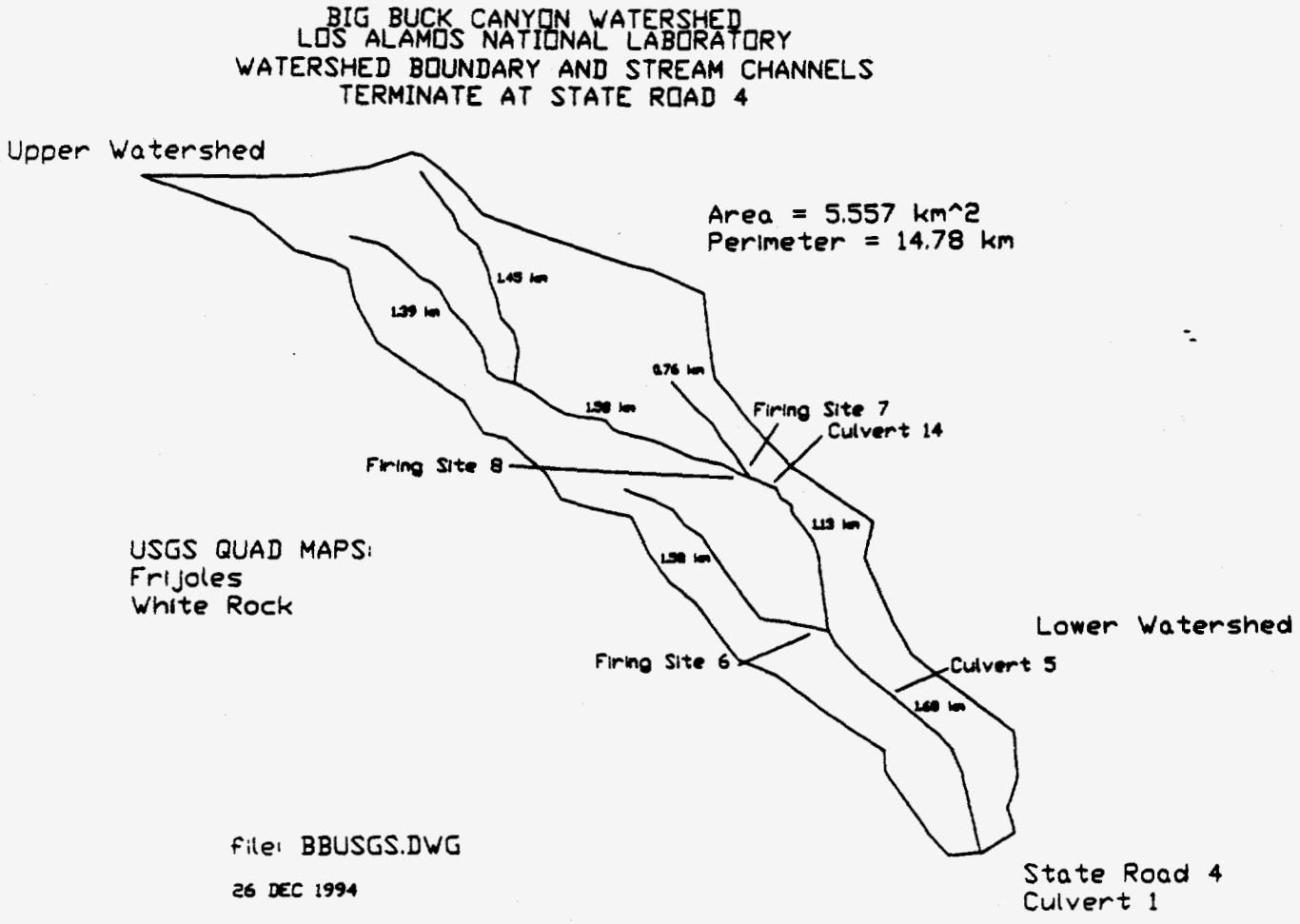

Figure 2
Big Buck Canyon Watershed

The main channel from TA-49 to State Road 4 is joined by three tributary streams. The "Saddle" tributary joins in the upper watershed, the Firing Site 7 tributary joins just downstream of Culvert 14, and the Firing Site 6 tributary joins the main channel at Culvert 12.

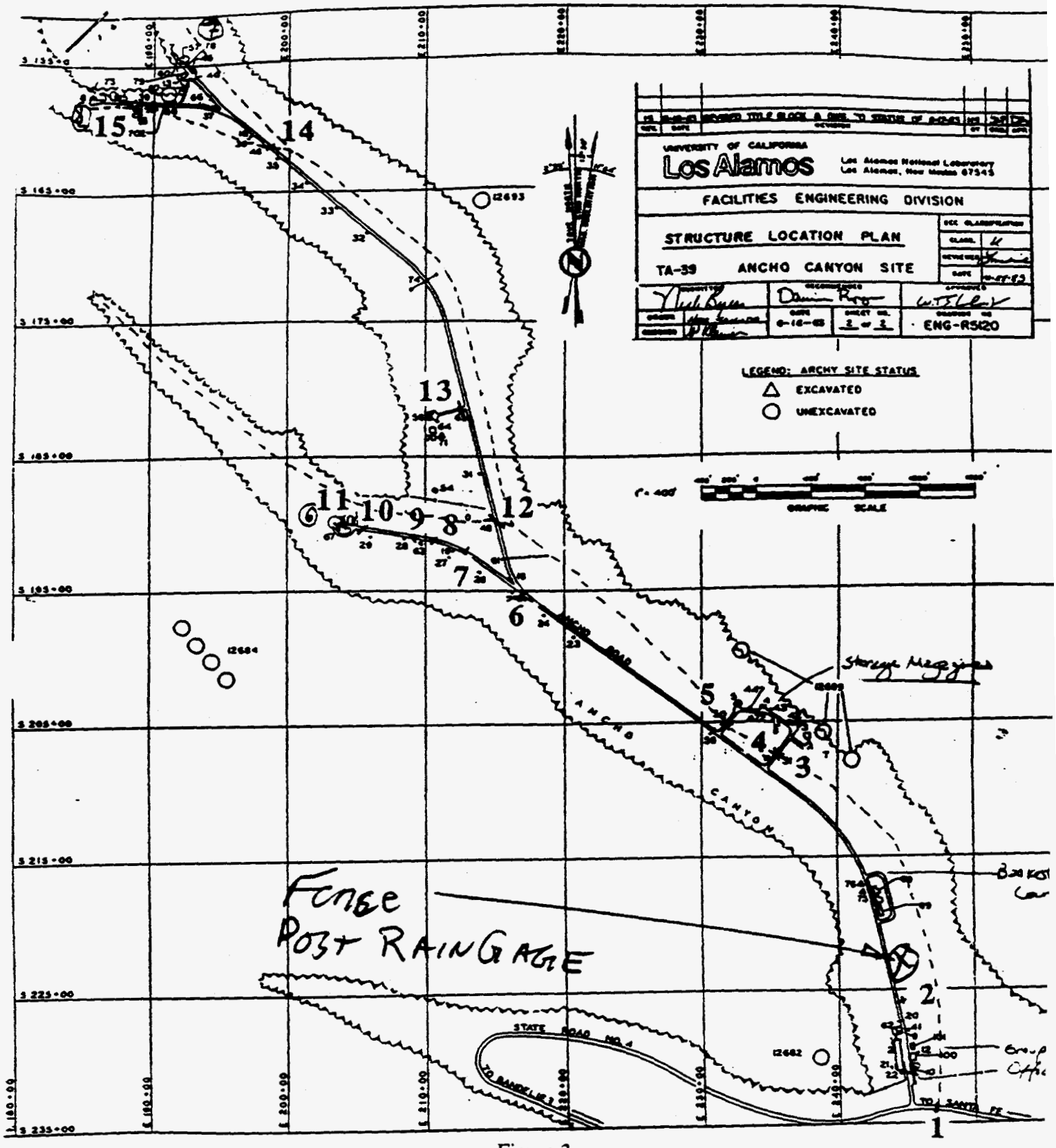

Figure 3

Locations of culverts and buildings in the lower Big Buck Canyon watershed.

Culvert 1, under State Road 4 is the end of the watershed. Stream monitoring stations are located at Culverts 5 and 14. The tributary flow from Firing Site 6 enters the main channel at Culvert 12.

example, to study the impact of hydraulic conductivity on the discharge rate, a physically based model is needed. Due to the ephemeral nature of the runoff process, all of the transport occurs in brief storm events. Therefore, an event oriented, distributed parameter, physical model was needed. The KINEROS program is one of this type. It was selected for application to Big Buck Canyon because it is designed to simulate the response of small watersheds to individual storm events, including the ability to predict erosion and sediment transport.

The KINEROS program is currently being revised and an interim version of the program is called KINEMAT. This transition version has updated rainfall and runoff algorithms but does not have the sediment transport features implemented. The fully revised KINEROS-II program should be released during the summer of 1995 and will include the modeling of sediment transport and erosion. Since the first step is to calibrate the rainfall and runoff processes, the present KINEMAT program was used to begin the modeling work.

1.4.3 Water Chemistry

Using channel sediment samples collected for Potrillo Canyon near Test Site E-F and near Skunk Works, Herrin (1994) measured the concentration of various metal associated with the sediment. He tested for uranium, lead, nickel, beryllium, barium, and cadmium. He also considered the leaching of metals into the dissolved phase while the sediments are in contact with water. While these samples were not collected in Big Buck Canyon, the results are assumed to be representative of how metals are mixed with and leached from sediments of this size and type.

1.4.4 Final Status of Research

The research is in progress with most of the effort directed at the development of the monitoring system and the formulation of the numerical model. Monitoring instruments have been installed in Big Buck Canyon at two locations along the main channel; however, the performance of the streamflow measurement system has yet to be proven by a runoff event due to the dry conditions since the installation of the equipment.

A numerical model of Big Buck canyon has been formulated and has been tested for sensitivities to various input parameters. The model calibration is limited due to the absence to runoff in Big Buck canyon since monitoring began in 1993. Qualitative calibration is being attempted using oral accounts of a large storm in 1991. When the fully revised version of the KINEROS-II program is available, the model can be substantially improved with compound channel cross sections, the definition of a grainsize distribution instead of a single median diameter, and a new soil physics based algorithm to redistribute soil water during an interruption in the storm using two soil layers. When a model is calibrated, a long term streamflow record can be simulated using historic precipitation data for the past several decades. Then streamflow frequency curves can be generated from the simulated record.

The final linkage between the movement of water and sediment and the movement of contaminants remains to be defined. Laboratory experiments by Russ Herrin measured the concentration of various metals associated with the sediments. The integration of the laboratory results with the modeling estimates remains to be performed.

interval associated with the large measured flood. This same concept of using simulated streamflow to construct a flood frequency relationship is proposed for Big Buck Canyon.

Hassan (1990) reports observations of desert flood bores in the Judean desert in Israel. He compared bore height with velocity and notice different bore characteristics depending on whether the stream bed is initially dry or wet.

The topic of transmission losses in the channel is addressed by a number of authors. Babcock and Cushing (1942) considered the infiltration into a desert stream in Arizona and proposed methods for increasing groundwater recharge by controlling the discharge of flood waters to maximize infiltration. They demonstrate the importance of a silt layer that impedes the infiltration. Burkham (1970) proposes a regression relationship between infiltration volume and inflow flood volume. Lane, Purtymun, and Becker (1985) present values for effective hydraulic conductivity for channels based on soil texture classes. For coarse sand, infiltration rate of 25 to 50 mm/hr are common. These numbers are based on a review of numerous ephemeral streams in Arizona, New Mexico, and Nebraska. A foot note in this report cautions that the effective value of hydraulic conductivity during a flashy sediment laden flood event is not the same as that determined by steady-state clean water infiltration conditions. Walters (1990) presents results for transmission losses for six arid channels in Saudi Arabia. All of these references, however, are based on water balance calculations using measurements at an upstream and downstream gauging station. None of them probe deeper into the underlying processes of infiltration into the coarse alluvial channel bed.

Walters (1988), however, does discuss the processes behind transmission losses. He has measured and modeled the movement of water into the soil after the passing of a flood wave over ephemeral channel beds in Saudi Arabia. Based on his observations, layers of fine grained materials control the effective infiltration rate even if coarse surface layers of sand have much higher hydraulic conductivities. In Big Buck canyon, the hydraulic conductivity was measured using the Guelph permeameter. The large values of hydraulic conductivity measured with the permeameter may not, however, be suitable to model the effective hydraulic conductivity that controls the transmission losses during an event.

1.5.2 Sediment transport in ephemeral streams

The transient rainfall-runoff response of ephemeral streams also impacts the sediment transport response. Equilibrium models of sediment transport are inadequate descriptions of the unsteady, discontinuous movement of sediment caused of brief, but intense, flow events. Laronne and Reid (1993) show pointed examples of how sediment movement in an arid watershed (Israel) is significantly different from that in a humid zone stream (Oregon, USA). Reid and Laronne (1995) further reinforce this concept with additional examples which bring into question the usefulness of currently available numerical models when applied to a problem like Los Alamos.

Laronne, et. al. (1994) explain why the typical layering of the gravel bed in a perennial stream is not characteristic of ephemeral streams. They show how streams in the Negev (Israel) do not generate an armor layer because of the high mixing of ephemeral flows and the absence of a baseflow to sort and winnow the bed material. The absence of an armor layer is one cause of elevated sediment loads in ephemeral streams.

Moore, and McMahon (1992a) are critical of physically based models citing some of the pitfalls; they include KINEROS among the models in their discussion.

Most of these researchers are principally concerned with hydrologic issues and do not address the added dimension of contaminants associated with the runoff water and sediment. The intent of this research is the integrate the hydrologic and chemical results to predict the transport of heavy metal contaminants. Lane, Purtymun, and Becker (1985), however, do connect these two areas using the concept of enrichment ratios. This research in Big Buck Canyon can also employ an enrichment ratio approach.

2. Experimental Field Work

There are two reasons for pursuing a strong effort in experimental field work. First, observations and measurements of the rainfall and runoff are the basis for understanding the physical process at work to erode and transport sediment. Second, the development, calibration, and evaluation of a numerical model must be founded upon measured field data. Thus, experimental field work is important for both process understanding and numerical modeling.

In Big Buck canyon, measurements of precipitation, streamflow, and suspended sediment are being made continuously using on-site battery powered dataloggers. A number of concepts are proposed to measure the scour of alluvial materials in the culverts and total sediment yield but these concepts have not been implemented. In support of the numerical model the channel was surveyed; soil samples were analyzed for grain size, porosity, and specific gravity; and hydraulic conductivity was measured in the field. Each of these topics will be explained in the following sections.

2.1 Precipitation Measurement

In Big Buck Canyon, precipitation is measured on the canyon floor using tipping bucket rain gauges. No measurements are being made on the mesa tops; however, the TA-49 meteorological station is on the mesa top just beyond the upstream end of the Big Buck watershed. Other sites of precipitation measurement in the vicinity are at TA-54, TA-6, and the Bandelier firetower.

2.1.1 Tipping bucket rain gauges inside the watershed

The tipping bucket rain gauges in Big Buck canyons are located beside culverts 5 and 14. The floor of the canyon extends half way up the watershed and Culvert 14 is located at the upstream end of the valley floor, near firing sites 7 and 8. This gauges is, therefore, close to the center of the watershed. Culvert 5 is approximately three quarters of the way down the watershed. The tipping bucket gauges are sensitive to even small amounts of rain. One tip of the bucket represents 0.01 inch of rain (0.25 mm). High intensity rainfall, however, may not be accurately measured. The gauges tend to under measure high intensity rainfall rates.

The datalogger is currently programmed to record the accumulated depth of precipitation every 15 minutes. I recommend that the program be changed to record the precipitation depth every 5 minutes. Due the rapid changes in precipitation intensity during a thunderstorm, a finer resolution of the rainfall would improve the modeling results. As the frequency of sampling increases, the volume of data also increases which makes data

2.1.4 Bandelier fire tower gauge

In addition to the weather stations operated by the Laboratory, there is a firetower located near the entrance to the Bandelier National Monument. A rain gauge on this tower is maintained in support of the National Atmospheric Deposition Program which collects rainwater samples for chemical analysis. This is part of a national study of acid rain. The raingauge is a weighing type with a recording pen on a paper drum (a Belfort rain gauge?). While this data is not in electronic form it is available as a hard copy of the pen plot.

The caretaker of the gauge has noticed that this location tends to be dry relative to the nearby gauges at TA-49 and at White Rock. The precipitation depth is commonly less at this site than at the others. For example, there was a large storm on 2 August 1991 (day 214) in which 1.76 inches of rain were recorded at TA-49; at the Bandelier Firetower only 0.68" were recorded. Thus the firetower gauge received only 38% of the TA-49 precipitation. This is only one event and, by itself, means little. It does; however, provide an example that confirms the caretaker's comment.

Note that this gauge, located on the Bandelier Firetower, should not be confused with the LANL weather station at TA-49 which is commonly referred to as the "Bandelier" station.

The gauge is outside the Big Buck watershed but is not far to the east of the tributary that flows past Firing Site 6. A sample of the data available from this site is included in Appendix H for the week including 2 August 1991. For more information, the caretaker, David Jardine, can be reached at (505) 667-3615.

2.2 Stream Flow Measurement

The flow of runoff water is measured at two culverts in Big Buck canyon, Culverts 5 and 14. The upstream culvert, Culvert 14, receives the runoff from the main contributing area in the upper watershed from TA-49 down to Firing Site 8. In the main channel after culvert 14, the tributary flow passing Firing Site 7 joins the main channel which continues downstream to the potential "sink" area. Just downstream of the sink, the tributary flow from Firing Site 6 joins the main channel which continues to Culvert 5 where the second stream monitoring station is located.

At both culverts 5 and 14 there are pressure sensors and a paddle wheel float to measure the flow. These two systems provide independent measures of the flow. The pressure sensors are, unfortunately, prone to a number of interferences that obscure the interpretation of the data. The paddle wheel float systems are simple and should be reliable, but since their installation, no runoff events have been experienced. Thus, the systems are unproven.

The streamflow measurements will be important for estimating the sediment transport capacity of the flow. The measurements will also be useful for calibrating and checking the performance of the numerical models.

2.2.1 Pressure sensors

Pressure transducers are mounted upstream and downstream of the culverts to measure the stream stage. A third pressure transducer is connected to a pressure sensitive plate filled with hydraulic fluid. This plate is called a total pressure cell. All three are attached to the concrete floor of the culvert and covered with 60 to 100 cm of sand since the stream bottom is higher than the culvert floor. From these three measurements is it is theoretically possible to calculate the depth of sand, the depth of flowing water, and the discharge rate. The idea behind burying the sensors was to protect them from debris washed downstream during a

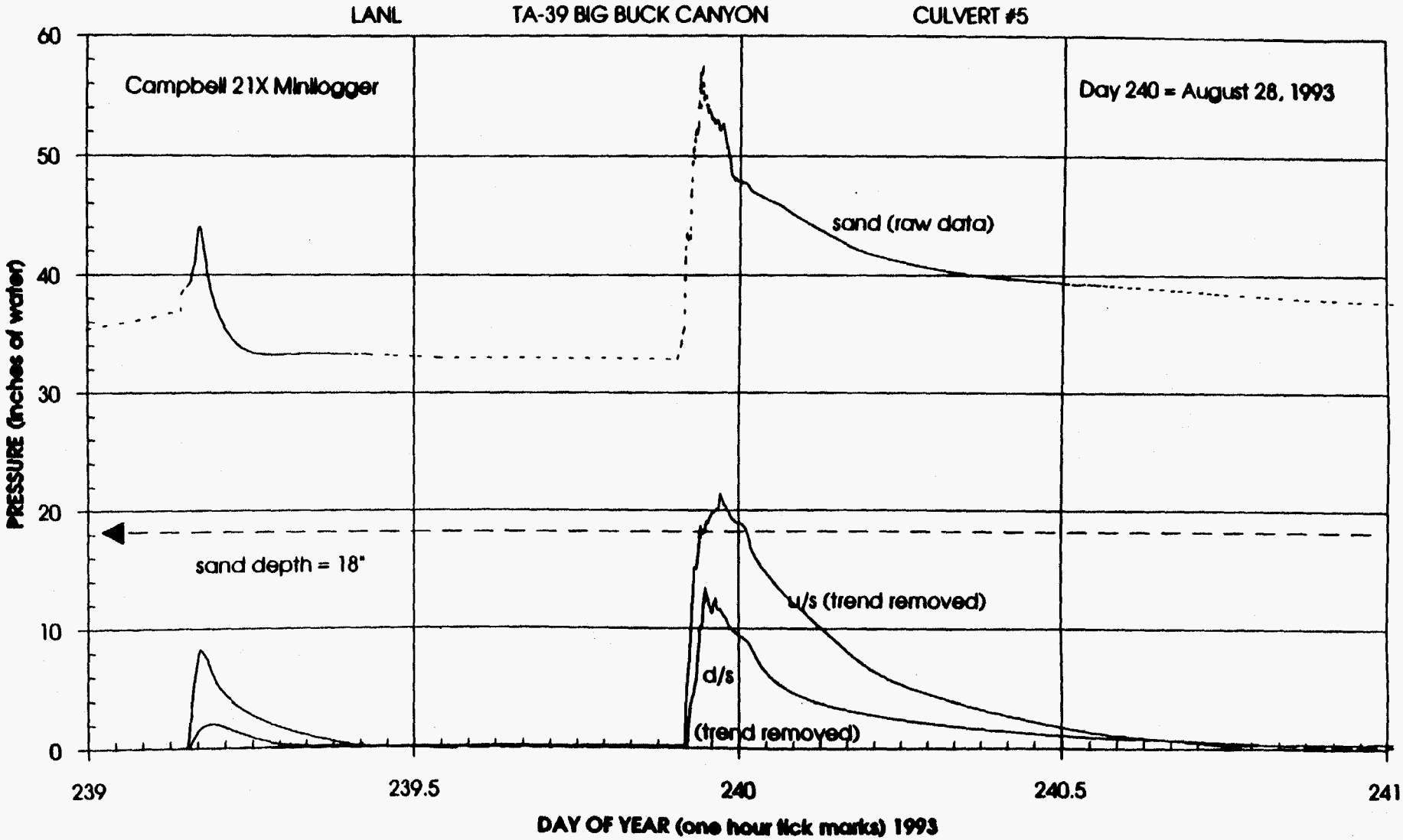

Figure 4

Pressure sensor measured hydrograph at Culvert 5, on 28 August 1993.

Sand depth is 18 inches. Upstream pressure sensor, labeled u/s (trend removed), only briefly measures stage above the sand level; most of the hydrograph is less than 18 inches which would indicate subsurface water. The downstream hydrograph, labeled d/s, is entirely below the sand depth.

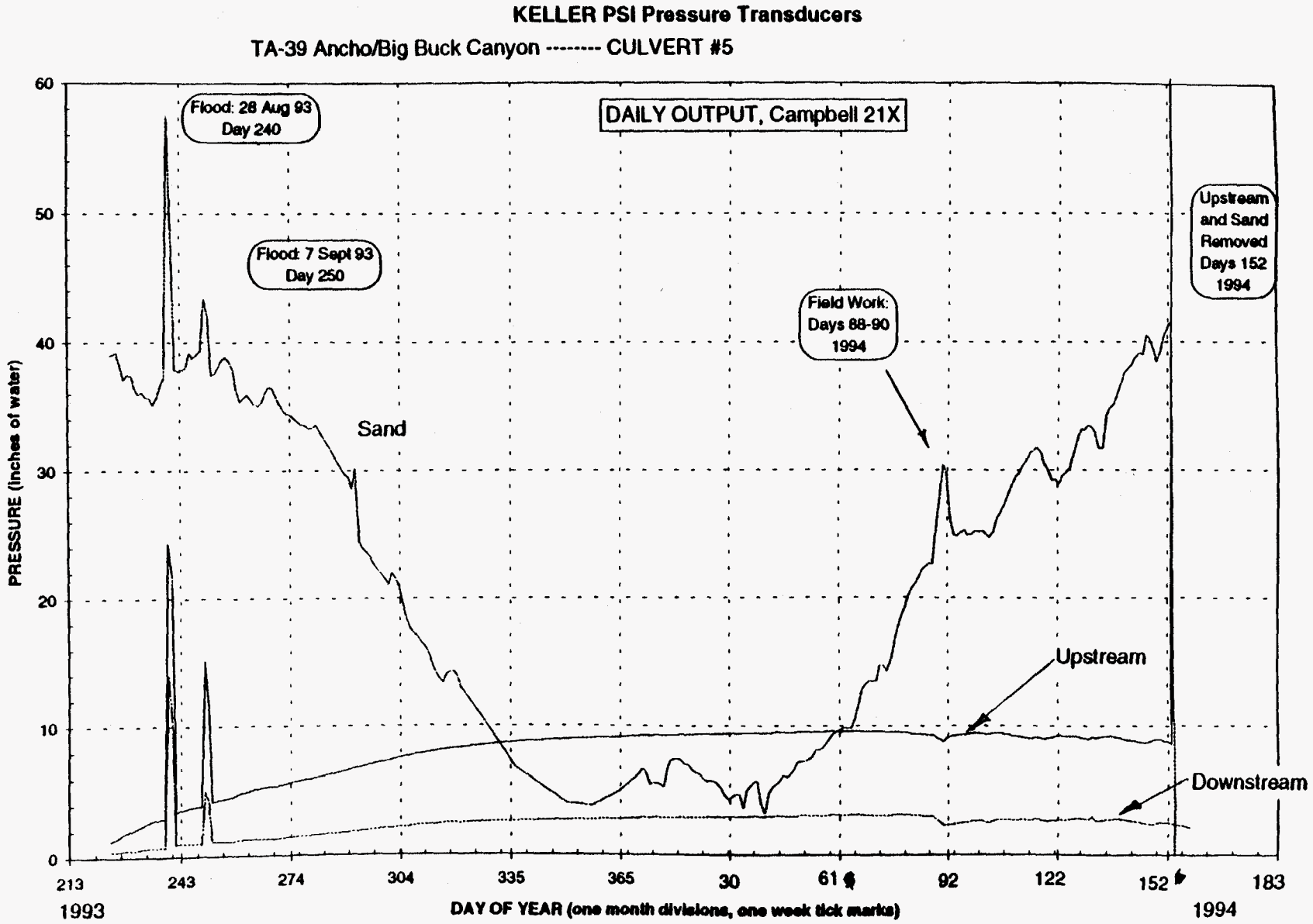

Figure 6
Long term zero drift in Keller pressure transducer signals

CAE,PERRY,I:\RALNL\DATALOGR\S5FILES.XLS

16 June 1994

2.5 Other Ideas Not Implemented

A number of other instrumentation concepts have been proposed. One of the chief short comings of the paddlewheel float measurement system is the potential scour of the channel bottom during a runoff event. The boom angle measures the elevation of the water surface, but the elevation of the channel bottom can also change. Two systems have been proposed to measure the location of the sand bottom. One is an acoustic sonar system attached to the bottom of the float and the other is a scour depth probe.

The acoustic system seems most promising. It consists of a small transducer mounted to the bottom of the float which is powered by the Campbell 21X data logger. The system is called an "up-looker sonar" because it is typically mounted to the bottom of a tank and beams a pulse of sound upward to the air-water interface. Common applications are water tanks and evaporation pans. In this application, the transducer will point downward to detect the sand-water interface on the bottom of the channel. Possible interferences may arise from air bubbles and suspended sediment in the flow, motion of the float on the surface, and poor definition of the bottom due to bedload mixing. The vendor, Global Water, was willing to sell a unit on a trial basis to test the performance of the sonar transducer under these conditions. The cost, approximately $1000, is also reasonable. The simplicity of the sonar system is a distinct advantage since it integrates easily with the existing paddlewheel float system and the Campbell 21X data logger.

A scour depth probe is an alternative means of locating the elevation of the bottom. This probe would periodically move down until hitting the sand, then retract to be clear of the flow and to avoid being an obstruction that would snag debris. The probe would be driven up and down by an electric motor and the reversing mechanism would be adapted from an automatic garage door opener controller. This is an active detection system that is power intensive. Providing adequate power is one of the design challenges associated with implementing this device. Normal 110 volt AC power is the best, but available powerlines are not easily accessed. It is possible to operate the system for a short period of time (1 hour) using a large 12 volt car battery equipped with a solar panel for recharging.

To avoid the power issue, a simplified version of the scour depth probe system could be built with a vertical pole mounted to the side of the culvert, free to slide down under the force of gravity while the sand bed under the foot of the pole is scoured away. A line attached to the top of the pole and wrapped around a pulley on a potentiometer would facilitate the measurement of the pole movement. This system could monitor the advancement of scour during the first part of a flood but would not be able to respond to the subsequent agradation of the channel bottom during the receding limb of the hydrograph. The maximum depth of scour and the time history of scouring down would be very valuable set of information even if the agradation process is not detectable. The system could be implemented for less than $100 and would be very simple to install. After a flood event. the probe would need to be dug out of the sand and reset to the surface before the next event.

Improvements in the measurement of flow would be beneficial, but improvements in the measurement of sediment movement could be even more helpful. The existing suspended sediment sampling bottle are simple but do not give insight into the time variation of the sediment concentration. Also, the bottles do not measure the process of bedload transport. Measurement of the total sediment load, and how it changes with time, would be a great advantage. Sediment is particularly difficult to measure, especially with automatic equipment that do not require a

While these values compare well to published values for coarse sand, Freeze and Cherry (1979) and McWhorter and Sunada (1977); they may not represent the infiltration rate during a transient flood event that is loaded with sediment. Lane (1985) recommends values for "effective" hydraulic conductivity in the range of 25 to 50 mm/hr; two order of magnitude less than the Guelph results. A note in Lane (1985) indicates that effective values of hydraulic conductivity are different than the values determined from steady-states infiltration experiments using clear water (which is descriptive of the Guelph method). The numerical model used the values determined by the Guelph permeameter; however, the simulation results suggest that these input values overpredict the transmission losses.

The Guelph permeameter proved to be an easy to use instrument capable of making fast samples; however, direct application of the Guelph values to a numerical model is questionable. Appendix B contains full results of the Guelph permeameter work and explains the calculation methods.

2.6.2 Grain size distribution, specific gravity, porosity

The soil samples collected from Big Buck canyon during the August 1994 field trip were analyzed to determine the grainsize distribution, porosity, and specific gravity. It was also possible to calculate the soil water content of the samples. Eight samples were taken from the surface deposits located in the channel, one sample was collected from an overbank zone, and one sample from the mesa top. The channel samples are composed of coarse sand while the mesa and overbank samples have significant fractions of gravel and silt/clay particles.

The channel samples were 7% gravel, 90% sand, and 3% silt/clay. The median diameter (D_{50}) was 0.9 mm. The overbank sample collected just upstream of culvert 12 was dominated by the sand fraction but with more significant gravel and silt/clay fractions. Gravel made up 24%, sand formed 62%, and silt/clay was 14% of the sample. This distribution is consistent with the soil survey results, Nyhan (1978), for Totavi gravelly loamy sand. The sample looked like medium brown dirt with scattered rocks and pebbles. The median diameter was 0.97 mm which is similar to the channel samples, however the variability in grainsize is much larger. When the mesa top sample was collected it was observed that there was a wide variety of soil structure types on the mesa top. Some areas were almost bare of soil with exposed rock outcrops. Other areas contained more soil and organic matter. The sample was contained 33% gravel, 57% sand, and 10% silt/clay; thus the distribution of the mesa top sample is similar to the overbank sample. The median diameter was 1.3 mm.

Relatively undisturbed soil samples were collected at eight locations for the analysis of porosity and specific gravity. The volume of each sample collected was 37.79 cm^3. Since the samples are composed mostly of sand and inorganic particles, it is assumed that the porosity and bulk volume did not change with drying the sample at room temperature. The mean specific gravity of the channel samples was 2.56 which is somewhat less dense than expected. Typically the specific gravity of quartz sand is 2.65.

The specific gravity of the overbank sample was 2.46 which is probably less dense due to more organic material. Lower density materials are more susceptible to erosion. It would be interesting to compare these values to the specific gravity of the Bandelier Tuff parent material. The Los Alamos Soil Survey (Nyhan 1978) did not have any values for specific gravity.

Survey (m) Chart 1

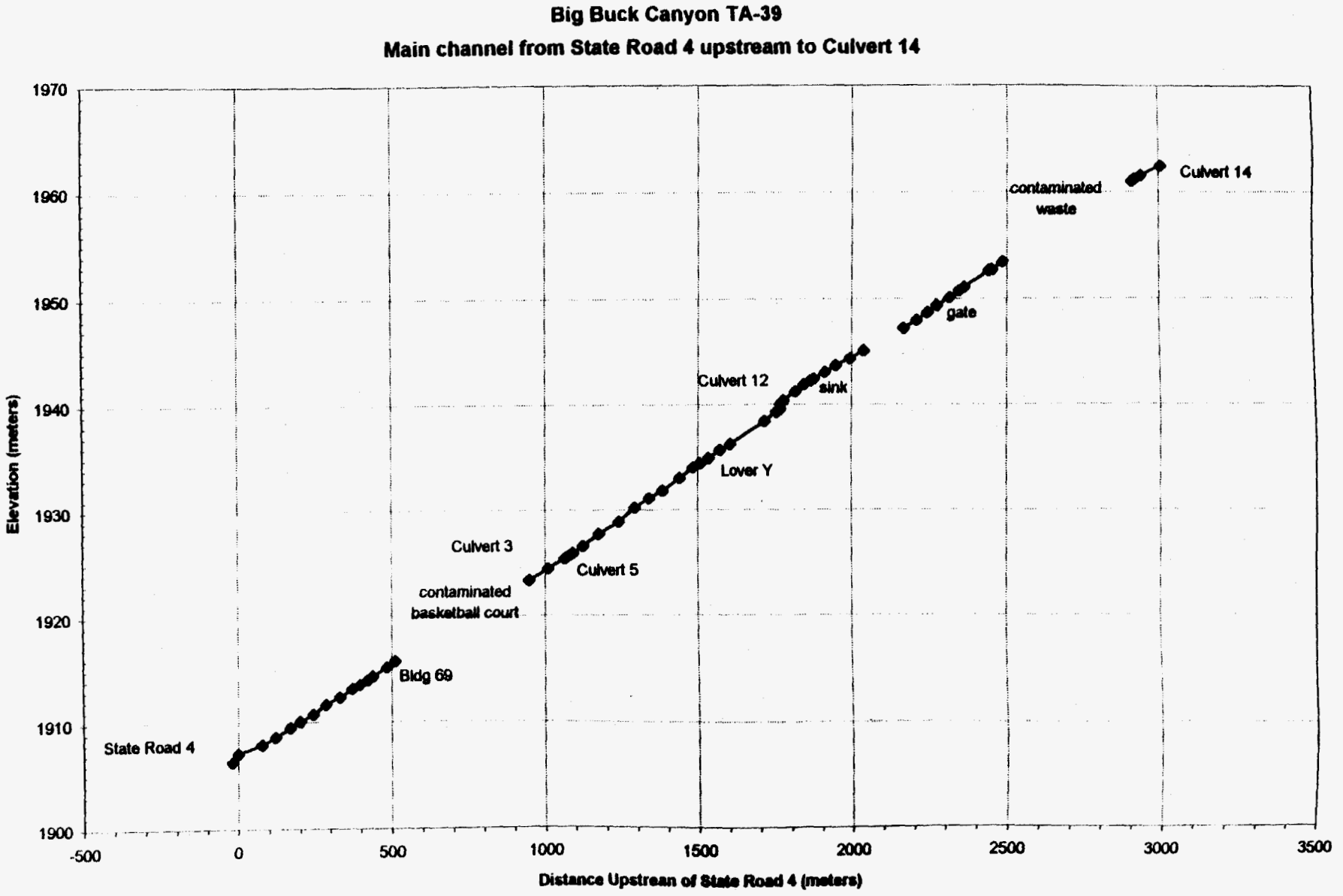

FIGURE 7

The USGS in New Mexico has developed regression equations for the state to calculate the two year flood discharge as a function of topwidth, which they call "active channel width." Using the USGS equation, the two year flood is 18 m^3/s. Accounting for the standard error in the regression, the flow is in the range of 10 to 20 m^3/s. The bankfull discharge estimate at this section of 11.9 $7m^3/s$ is compatible with the USGS estimate.

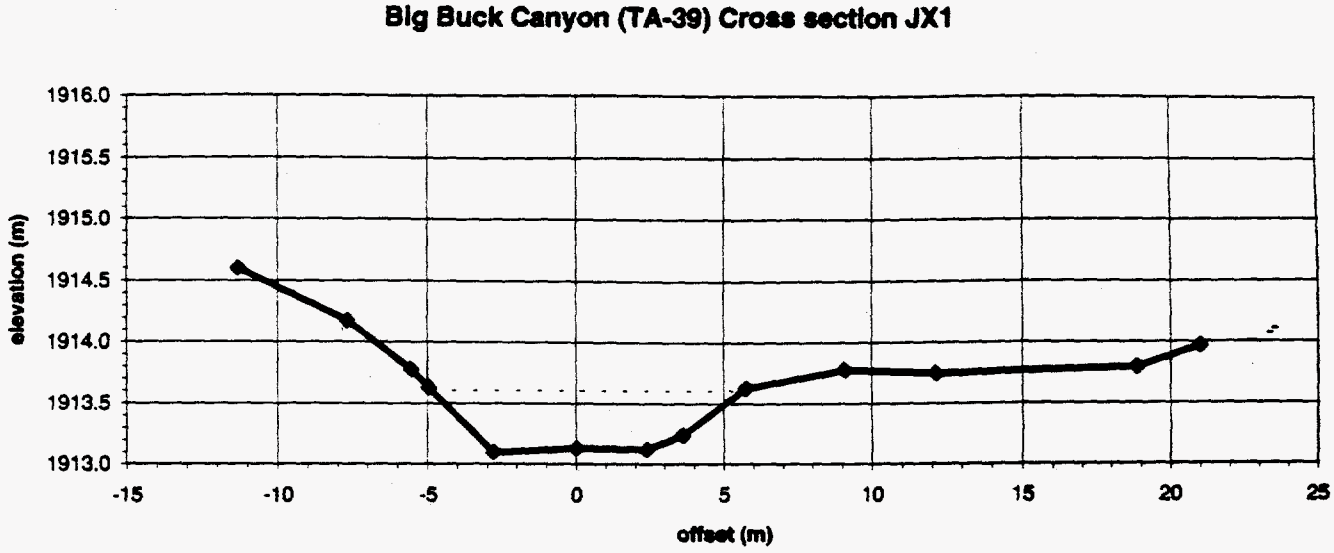

Figure 9
Cross section JX1 looking downstream
Located 372 m upstream of State Road 4, cross section JX1 is just upstream of the TA-39 group office building. Bankfull discharge is in the range of 8.5 to 11.9 m^3/s depending on roughness assumptions.

Table 2
Bankfull discharge estimates at surveyed channel cross sections

Cross section	Location	Bottom Width	Top Width	n = 0.025 $Q_{bankfull}$	n = 0.035 $Q_{bankfull}$
JX1	372	5.18	10.68	11.9	8.5
JX2	440	3.96	11.40	21.5	15.4
D/S culvert 5	1042	3.71	13.83	12.6	9.0
U/S culvert 5	1124	3.28	6.15	4.3	3.1
KX1	1294	7.01	13.41	17.7	12.6
MX1	1507	2.07	6.74	10.9	7.8
QX1 discharge sink	1876	18.08	22.55	7.0	3.5

3.1 Model Selection Criteria and Recommendations

Though the principal goal is to address the problem of contaminant transport, the immediate task is to model the rainfall, runoff and sediment transport processes. Therefore, the modeling criteria do not emphasize contaminant transport but instead focus on the hydrologic and geomorphologic processes. In order to estimate the movement of water and sediment, a suitable model must have characteristics that apply to the environment and scales of interest at Los Alamos. The most important characteristics are the geometric scale and kinematic scale of the model.

Six specific criterion were used to evaluate potential numerical models. The first criterion is that the model must be valid on a 5 km^2 watershed. Second, a short time step on the order of one minute is needed to simulate storm durations of a few hours or days. Third, precipitation input must be distributed in space and time. This points to a fourth selection criteria; the model must define distributed soil properties that can replicate the channel transmission losses and model the discharge sink dynamics. Fifth, the model must be able to simulate ephemeral streamflow in a network of channels. And sixth, the model must simulate sediment movement as a function of the soil characteristics

Models were classified into general approach strategies for systematic comparison. The approach types are:

A) Residence time models
B) Watershed scale process models
C) Small scale process models

Residence time (transfer function) models relate the material output from a system to the material input and a set of parameters that characterize the response of the system. The system may be a single deposit, a portion of a basin (such as a stream channel), or the entire watershed. The transfer function can be derived in a number of ways: by postulating a mechanism in the system (such as plug flow or completely mixed), by statistical observations (such as regression or auto regressive moving averages), or by applying a process model to a particular system.

Watershed models (also called distributed parameter, physical models) estimate the material output from a system (and at points within the system) given various inputs to the system by transporting through and transforming within the basin the added material, or material stored in the system. Such models utilize the conservation laws of mass, momentum, and energy, and physically based process relations. The size of the system is defined by the boundary of the watershed.

Small scale models utilize a similar physical approach as watershed scale models; however, the system of interest is a local region within the watershed (such as a firing site, a waste storage site, or a discharge sink). The model results from these critical areas can then be integrated into the appropriate subunits in the watershed scale model.

Of the dozens of watershed scale models considered, two are recommended - KINEROS and HSPF. Because of the spatial distribution of parameters in KINEROS, particularly the input from many rain gages, and the history of application of the program to ephemeral, arid watersheds, this program appears to be the best choice for the study of Big Buck Canyon. KINEROS is single storm event oriented and does not support continuos simulation of the water budget.

Hard copies of these files are in Appendix G and electronic copies are on the enclosed floppy diskette in the subdirectory A:\KINEMAT

3.2.1 Input geometry, soil parameters, and hydraulic parameters

Big Buck canyon drains to an outlet culvert under State Road 4 (Culvert 1). The drainage area above Culvert 1 is 5.54 km^2. Photo topographic maps were used to mark the watershed boundary and subdivided areas. The overall basin area was checked by independently outlining the watershed on USGS 1:24,000 quad maps and measuring the basin area. The area determined using both map sources agreed within 0.2%.

KINEROS provides five element types; planes, channels, pipes, detention ponds, and a composite urban element type. I am modeling the mesa tops, canyon walls, and valley floors with plane elements. The channel reaches used channel elements. In addition, to represent the constriction in the channel provided by the fence just before State Road 4, I have defined a pond element. No pipe or composite urban elements have been employed.

The drainage area has been subdivided into 66 model elements. Figure 10 is an AutoCAD drawing of the watershed and modeling elements. This drawing was constructed by digitizing the element areas drawn on the photo topographic maps. This drawing was also used to measure the areas of the elements and to locate the element centroids.

Model elements were chosen to provide information at selected locations along the channel. Significant locations along the channel include points where tributaries contribute, stream gauge locations, and changes in channel slope. From upstream to downstream along the main channel the main locations are: TA-49 mesa, saddle tributary input, firing site 8, Culvert 14, firing site 7 tributary input, discharge sink, Culvert 12 tributary input from firing site 6, Culvert 5, the fence, and Culvert 1 under State Road 4. The location, elevation, and channel width at each of these points along the main channel are listed in Table 3.

Table 3
Important locations along the main channel

Location	Main Channel Location (m)	Elevation (m)	Slope %	Main Channel Bottom Width (m)
TA-49 Mesa Upstream end of channel	6100	2100	4	1 approx
Tributary from Saddle	4650	2045	6	1 approx
Firing Site 8	3460	1968	2.0	2 approx
Culvert 14	2910	1961	1.8	2
Discharge Sink	1850	1942	1.7	18
Tributary from Culvert 12 and Firing Site 6	1756	1939	2.2	10.1
Culvert 5	1081	1925	1.9	4.5
Fence	76	1908	1.1	1.3
Culvert 1, State Road 4 Downstream end of channel	0	1907		5

Once the channels are subdivided into reaches, contributing areas to each channel element are delineated by working up hill to the watershed divide from the downstream end of each channel reach. These contributing areas are further subdivided into reasonably homogeneous planes that drain from one to the next towards the channel. The choice of elements is largely determined by changes of slope that are apparent on the photo topographic maps by the closeness of the contour lines, shading, and vegetation cover. The subdivision choices were made by visual inspection. The three groups of plane elements are overbank valley floors, steep canyon walls, and mesa tops. The range of slopes for mesa top elements is from 5% to 25%, for canyon wall elements is from 33% to 96%, and for valley floor elements is from 0 to 10%. The vegetation patterns closely follows the slope groups; it is, therefore, assumed that the soil types also follow the slope groups.

All of the mesa elements use the same soil parameters. Likewise, all of the valley floor elements use the same set of soil parameters. These input parameters are listed in Table 4 for mesa, wall, floor, channel, and pond elements. The parameters include Manning's roughness "n" values, interception depth, vegetative cover, and soil properties. The soil properties include saturated hydraulic conductivity, effective soil capillary drive, porosity, maximum saturation fraction, and volumetric rock fraction. The KINEMAT input parameter variable names will be listed in all capital letters. For example, Manning's number "n" is called MANNING in the KINEMAT input file. The Manning's roughness value (MANNING) was set to 0.035 as an initial first guess. This value should be improved.

The interception depth (INTER) was set to zero, as was the value for vegetation cover (COVER). These zero values should not be significant due to the relatively sparse vegetation. The zero values will increase runoff compared to non-zero values. Typical values of vegetation cover are probably on the order of 30%.

The saturated hydraulic conductivity is the asymptotic infiltration rate as the duration of the precipitation increases. A zero value can be used to define an impervious area. For example, the detention pond hydraulic conductivity was set to zero. The infiltration capacity of the soil is governed by several input variables (hydraulic conductivity, effective capillary drive, fraction of rock in the soil volume, porosity, and initial soil moisture content). By setting the initial soil moisture to 100% in the "run" file, the infiltration during the full duration of the simulation is controlled by the hydraulic conductivity and not by capillary effects.

Hydraulic conductivity (KS) is a very sensitive input parameter, especially for the valley floor and channel elements. In these two areas, the hydraulic conductivity was measured in the field using a Guelph permeameter. Whether the values measured are representative of the effective infiltration rates experienced during a runoff event is an area of question.

The effective capillary drive (G) is the inverse of the alpha parameter used in the discussion of the Guelph permeameter by Elrick (1987).

$$G = \frac{1}{\alpha^*}$$

Input values were based on information found in the literature for alpha values. Elrick (1989) cites a value for sand which was used for the channel and a value for loam used for the valley floor. Gallaher (1993) cites a value which was used for the mesa top. In the actual

The hydraulic conductivity of the channel and the overbank valley floor areas are two very important the parameters. The calibration of the model will likely center on a suitable choice for these values. This is unfortunate since the idea behind a distributed physical model is that input parameters can be measured independently in the field and input into the model. The model should then produce meaningful results without further adjustment. If the model parameters must be calibrated by the model itself to produce results that are consistent with observations, two things are indicated. Either the model fails to represent the processes at work in the field or the measurement does not adequately describe the property intended by the input variable. This is not an uncommon situation. Most measurements are "point" values that represent a spatially variable field. The hydraulic conductivity of a point may not adequately describe the variation of hydraulic conductivity throughout a sub-area element. The other issue of whether the model faithfully represents the dominate processes at work in the field is also a critical matter that will be investigate latter in this report.

3.2.2 Input precipitation data

The KINEMAT input file for precipitation can include as many as twenty rain gauges. The location of each gauge defined and the precipitation is input as a cumulative depth time series. The model is event oriented, meaning that the precipitation input defines one particular storm. Each storm requires a separate set of precipitation inputs and initial conditions; contained in a set of *.PRE and *.RUN files.

The present network of rain gauges is composed of tipping bucket gauges in the watershed and the LANL weather stations nearby. The most recent large event was a flood in August of 1991, before the tipping bucket gauges were installed. Data for this event is available on-line through the LANL common file server (CFS). ~~The procedure for securing this data and~~ the syntax of the files is documented in Appendix H.

The LANL weather station data at TA-49 and TA-54 Area G were obtained and filtered with a small FORTRAN program to extract the 15 minute precipitation data. The data was then totaled to create the cumulative rainfall time series suitable for input to KINEMAT. The filter programs are called FRTA49.FOR and FRTA54G.FOR to extract the rain gauge data from the larger file of meteorological data. The program to generate the cumulative time series is called PRECUM.FOR. ~~All of these programs are documented in Appendix H.~~

The assignment of weighting factors for each rain gauge to each model element is accomplished automatically using the input coordinates of the gauges and element centroids. The KINEMAT program determines the proximity of each element the surrounding gauges and applies weighing factors appropriately. The user can override the program weightings with manual inputs if desired.

The date of the event is not known. Naomi Becker has recorded the date to be 15 August 1991; however, this is very unlikely based on an inspection of rain gauge data on that date (Day 227). Only 0.02 inches were collected at TA-49 and the day before was dry. The other gauges at TA-6, TA-54 Area G, and the Bandelier Firetower showed similar patterns. Even on the next day, less than 0.19 inches were collected at any of the gauges. Table 5 contains the daily totals at all of the stations for three selected dates.

simulation. Model precipitation inputs from the TA-49 and TA-54 Area G weather stations were assigned to each model element according to the proximity to each rain gauge. In general, the upper watershed was strongly influenced by the TA-49 gauge which had heavy rainfall while the lower watershed was more influenced by the TA-54 Area G gauge which had much less rainfall. Figure 11 is a plot of the cumulative rainfall depth at the two gauges.

The simulation time began at 17:00 and continued for 120 minutes. The time step was 1 minute. Notice that the precipitation pattern at both gauges was similar during the first 30 minutes, then the rainfall rate at TA-49 increased dramatically to 64 mm/hr during the second half hour of the simulation. Both gauges show that very little additional rain fell during the second hour.

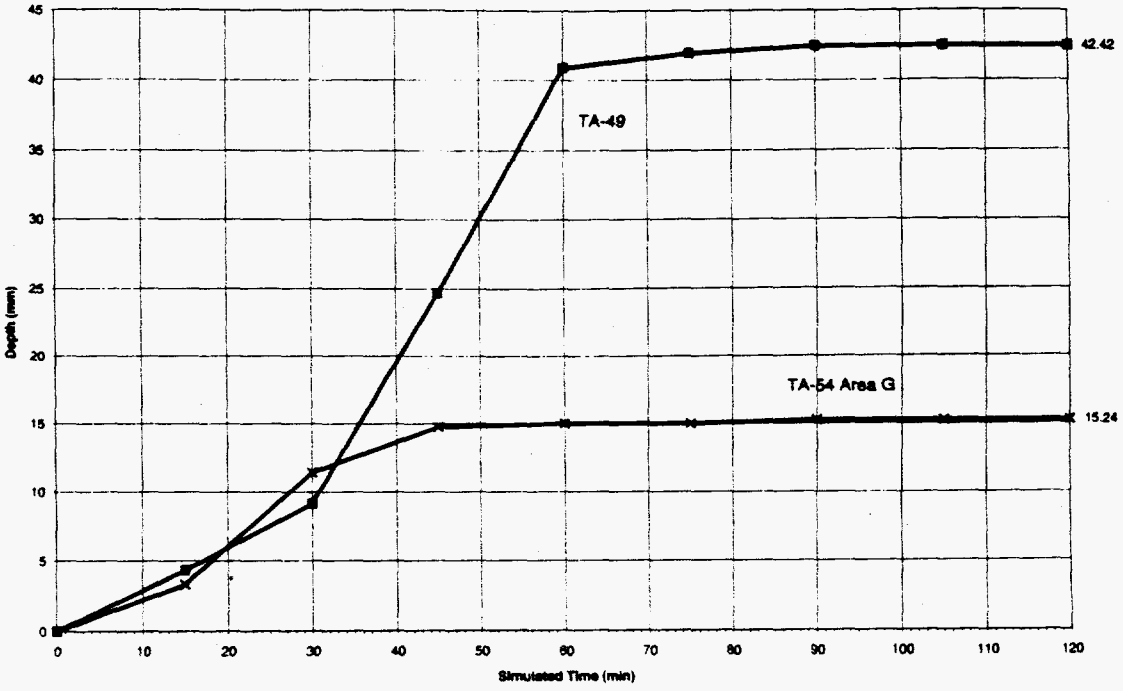

Figure 11

Precipitation Input from TA-49 and TA-54 Raingauges

Cumulative precipitation depth records from the LANL weather stations at TA-49 and TA-54 Area G on 2 August 1991 (Day 214). Simulated time t=0 begins at 17:00. Peak rainfall intensity at TA-49 during the second half hour of the simulation was 64 mm/hr.

The response of the watershed will be view in three areas: the upper watershed area, the lower watershed overland flow area, and the lower watershed main channel flow. The upper watershed is close to the TA-49 rain gauge; consequently, the hydrograph response in the upper watershed reflects the intense burst of rain during the second half hour. Figure 12 shows four hydrographs in the upper watershed. The flow off of the mesa top plane, element

1, is the first to respond to the precipitation pattern, but the volume of this hydrograph is small. Further down the channel, additional area contributes to the flow. At Firing Site 8 the hydrograph is at a maximum with a peak discharge of 14 m^3/s. A short distance downstream, at Culvert 14, the hydrograph has already begun to attenuate due to transmission losses in the channel. Between Firing Site 8 and Culvert 14 the channel slope is approximately 2% which is flatter than the reaches above that, which range in slope form 4 to 6%.

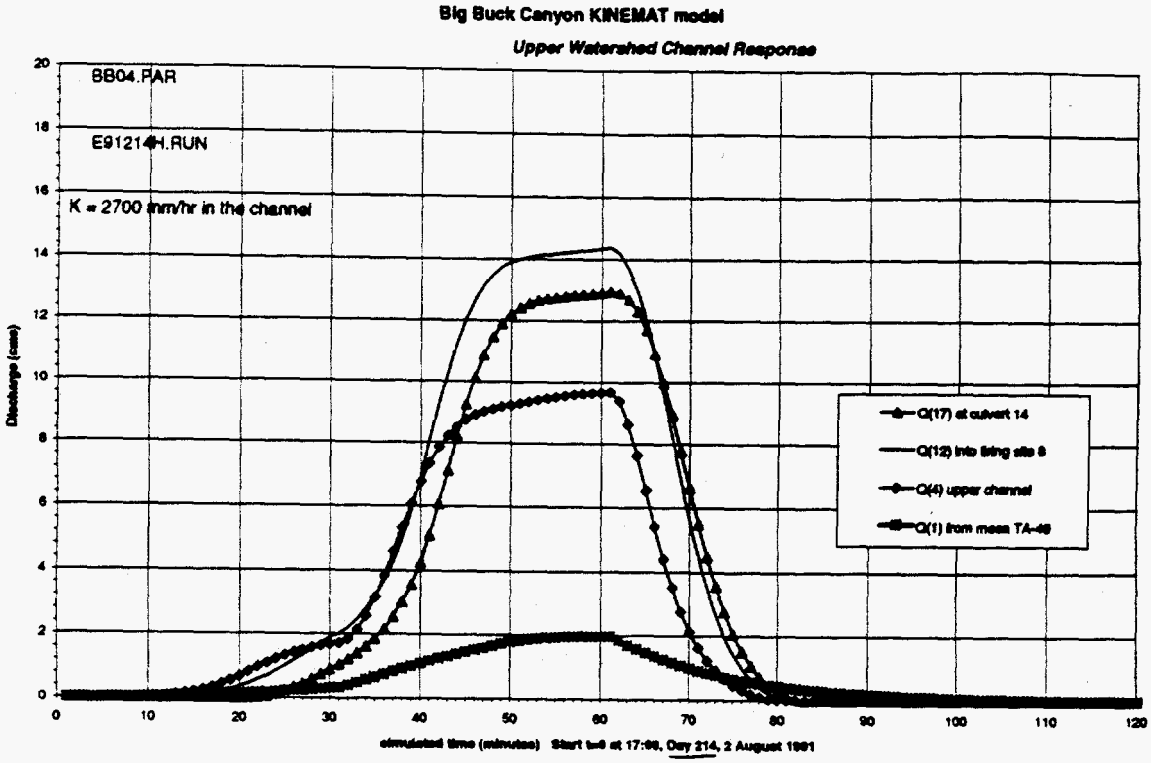

Figure 12
Simulated upper watershed response hydrographs
Flow on the mesa top plane (element 1) closely follows precipitation input pattern. Flow increases downstream to firing site 8. High transmission losses reduce the flow between the firing site and Culvert 14, where the gradient of the channel flattens out.

The overland flow in the lower watershed was very small due to the moderate rainfall at the TA-54 Area G gauge. A sample series of hydrographs from the mesa, down the wall, to the canyon floor is shown in Figure 13 for elements 45, 46, and 47. All of the runoff from the mesa and the wall infiltrated in the canyon floor element which has a relatively high hydraulic conductivity (160 mm/hr). No water reach the main channel. While this is undramatic, it

does simplify the interpretation of the transmission loss process in the main channel because the lower watershed did not contribute as a lateral input to the main channel flow.

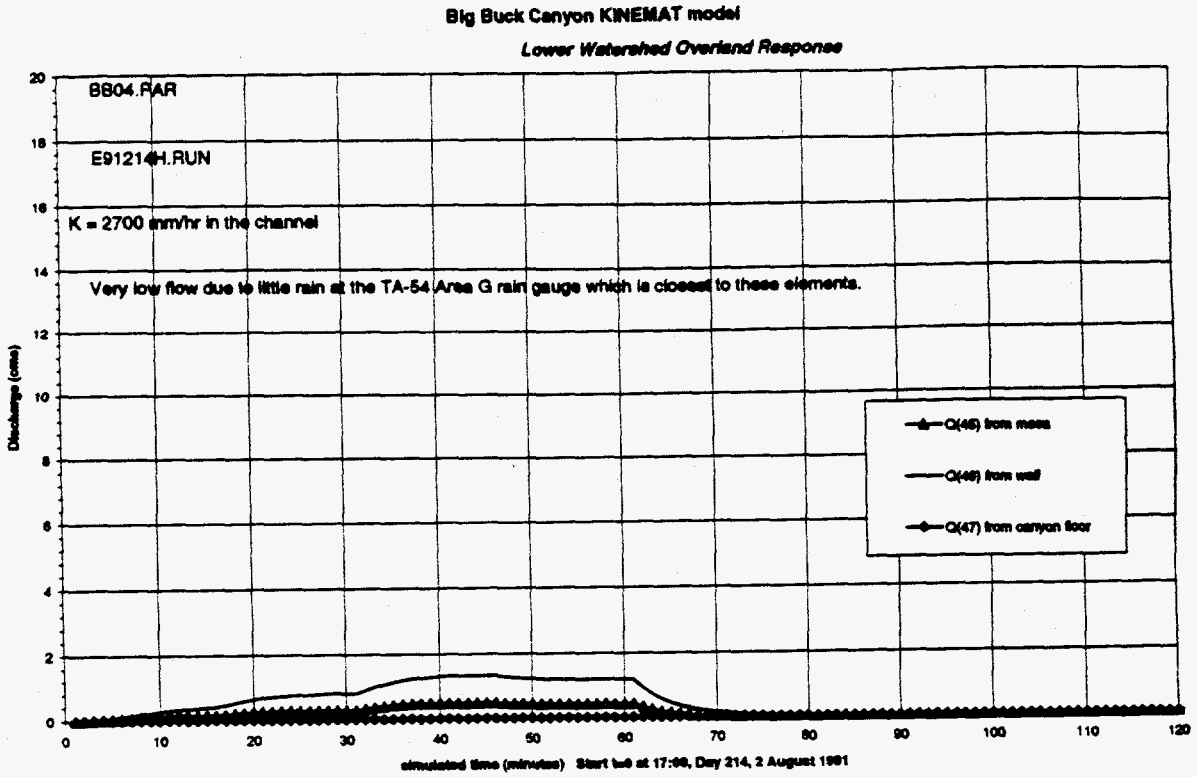

Figure 13

Lower Watershed Overland Flow Response

Flow over mesa top planes, canyon walls, and canyon floors are small compared to the upper watershed response since these elements are closer to the TA-54 rain gauge which has less precipitation than the TA-49 gauge. The lower watershed did not contribute to flow in the main channel.

The transmission losses in the main channel are clearly demonstrated by the series of five hydrographs in Figure 14. The flow from the upper watershed, out of Culvert 14, is routed down the main channel and first encounters the sink area. Although the sink in not long in length the extra width of the channel (if it can be called a channel) through the sink attenuates the peak discharge from 11 m^3/s at the inlet to 9 m^3/s at the outlet. The flow continues to diminish in terms of volume and peak rate until it is only 1 m^3/s when passing the group office

and entering the pond element. This dramatic decrease in the size of the hydrograph is a function of the hydraulic conductivity of the main channel which was 2700 mm/hr.

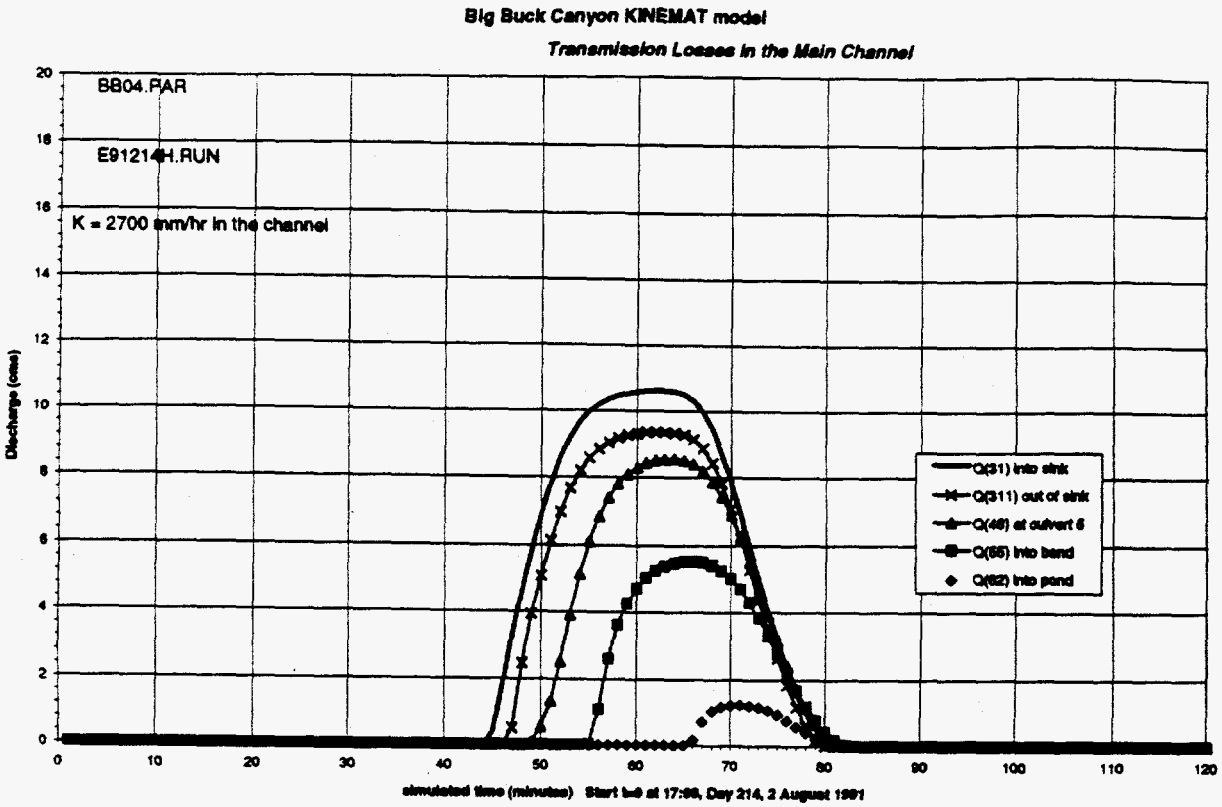

Figure 14

Transmission Losses in the Main Channel

The flow is attenuated in the downstream direction in the main channel due to high transmission losses. The flow past the discharge sink is reduce due to a wide channel for a short distance. The flow is steadily reduced along the length of the channel. From Culvert 14 to the inflow to the pond, 90% of the flow volume is lost to infiltration in the alluvial channel bed.

Observed accounts of the event by on-site employees have been collected by Naomi Becker and are summarized as follows:

- Water levels up to the hub caps on a large truck in the parking lot near the group office.
- Foundation of the group office building (Building 100) was partly eroded.
- Foundation of the shop building near Culvert 3 partly undermined.
- The road was damaged by main channel downstream of Culvert 12. The subsequent repair included moving the main channel further over toward the canyon wall, thus creating the present island of trees bounded by the old channel and the new channel.
- The channel was further stabilized upstream of Culvert 5 after the event to protect the road and guide the flow into the culvert.
- The flow moved in surges, or pulses, or waves down the channel that could be heard by a roaring noise; possible evidence of roll waves.

- At least an inch of rain fell in less than a one hour period.

These observations can be used for checking the model performance. For example, the constriction caused by the security fence just downstream of the group office was a likely cause of the elevated waterlevels which flooded the parking lot. The channel, which is typically 4 to 5 meters wide, must pass through a narrow opening under the security fence that is only 1.3 m wide. In spite of this backwater effect, the velocities near the group office were still sufficient to scour and undermine part of the foundation of the building. Rip rap has subsequently been installed to protect the building in the future. The erosion of the foundation is also evidence that the flow was out of the channel banks.

Bankfull discharge estimates and the USGS regression equation for the two year flood magnitude are independent values useful for assessing the model results. The bankfull discharge estimated at two cross sections in this reach of channel is in the range of 8 to 22 m^3/s depending on the assumed roughness and bankfull elevation. The USGS regression is based on the topwidth of the active channel, which in this reach is approximately 10 meters. The USGS regression estimate of the two year flood discharge rate is 18 m^3/s.

The KINEMAT model simulated a peak flow rate of only 1 m^3/s past the group office which is much less than the bankfull estimate. This indicates that the input value for hydraulic conductivity is too large. The effective infiltration rate must be less than 2700 mm/hr to match the observed response in 1991.

3.3.2 Model sensitivity to input parameters

The sensitivity of the simulated results to various input parameters was compared using the flow at the downstream end of the watershed (element 62) as the location of interest. This is just before the pond element and represents the flow in the area of the group office (building 100).

The most sensitive value governing the discharge volume and peak flow rate is the hydraulic conductivity of the channel elements. This value determines the transmission losses that can significantly attenuate the flow as it advances through the watershed. The hydraulic conductivity of the soils in the main channel was measured using the Guelph permeameter; the mean value was 2700 mm/hr. This values was used in the base case simulation above which demonstrated the impact on the hydrographs shape at various locations along the length of the canyon. From the literature, typical values for the effective hydraulic conductivity in sandy channels are two orders of magnitude less than the value measured with the Guelph. Thus a set of runs using channel hydraulic conductivity values of 2700, 270, and 27 mm/hr were run; the resulting hydrographs are shown in Figure 15. All of these cases assumed initially saturated soil conditions.

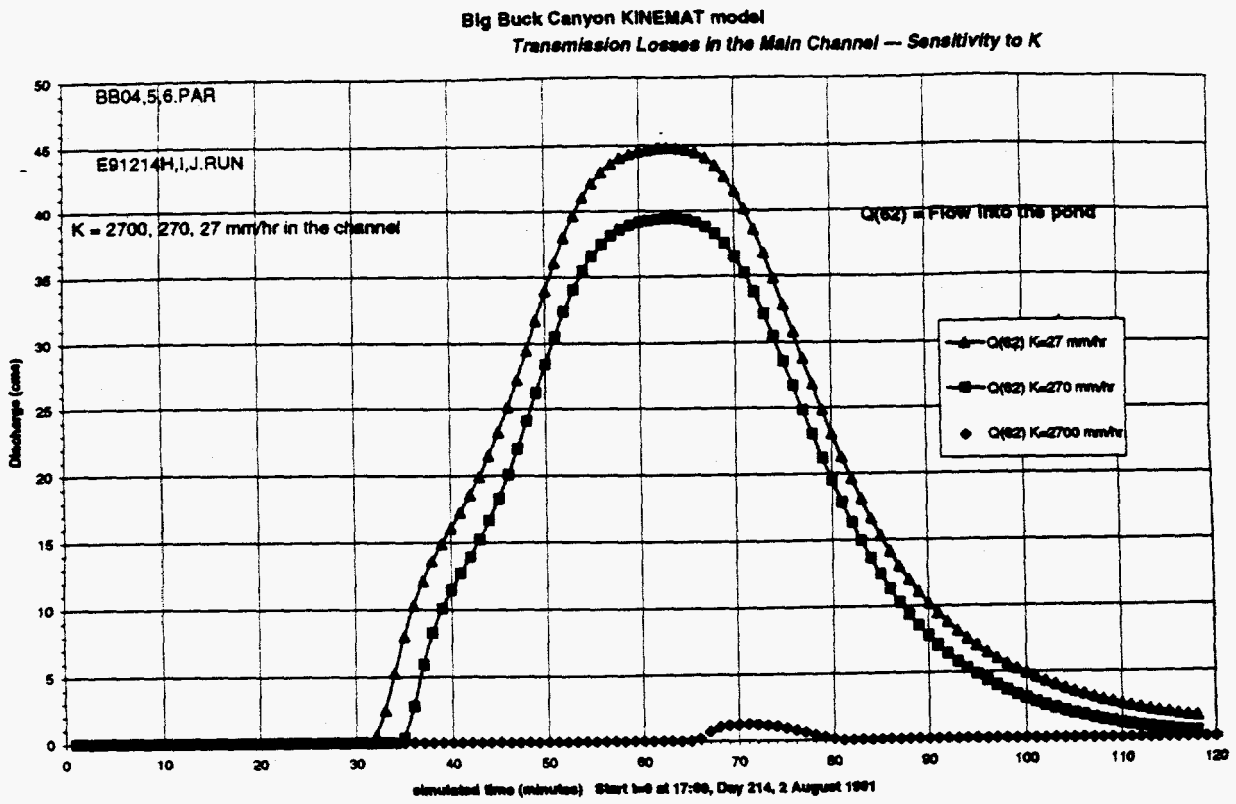

Figure 15

Sensitivity of Hydraulic Conductivity of Channel Elements

A high value of hydraulic conductivity can significantly attenuate the hydrograph at the downstream end of the watershed. Using the 2700 mm/hr value for hydraulic conductivity, determined by the Guelph permeameter, almost all of the runoff volume is taken up by transmission losses and little exits the watershed.

The sensitivity to the initial soil moisture was expected to be significant and it was. The base case presented above assumed saturated initial soil conditions (Si = 1.0). Three additional runs considered unsaturated conditions by assuming values for initial soil moisture of 0, 0.5, and 0.8. The discharge volume at the end of the watershed is twice as large when the soil is initially saturated compared to initially dry. Figure 16 shows a breakpoint in the response curve near the initial saturation value of 0.5. Below this value the response is similar to the dry conditions. Above 0.5 the volume increases steadily to a maximum when the soil starts out saturated.

The initial soil moisture is an input value in the KINEMAT .RUN file. Each element in the model can be assigned a unique value, but for this sensitivity test, all elements were assigned the same value for initial soil moisture. The discharge volume is also a function of the hydraulic conductivity of the main channel; for these cases the hydraulic conductivity was 27 mm/hr.

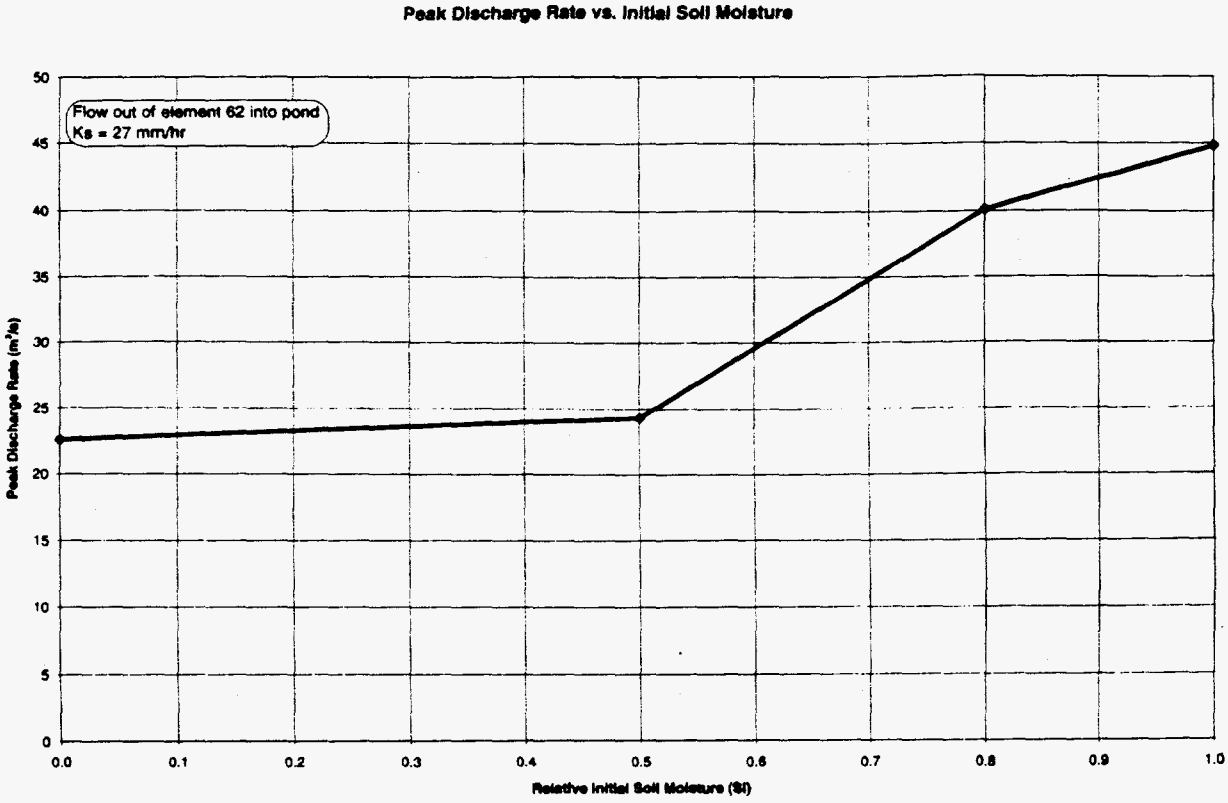

Figure 16

Sensitivity to Initial Soil Moisture Input

Discharge volume is twice as large when soil is initially saturated compared to initially dry. Relative soil moisture is the fraction of the pore spaced filled with water (Si=0 means dry, Si=1.0 means saturated). Based on the 2 August 1991 event, with hydraulic conductivity in the channel = 27 mm/hr.

Hydraulic roughness, expressed in terms of the Manning's "n" value, is not a sensitive parameter in the simulation of the watershed response. Figure 17 shows three hydrographs for the flow at the end of the watershed. The base case used a value of 0.035 for all elements. Two additional cases considered the effect of a rougher model (n=0.045) and a smoother model (n=0.025).

The hydraulic roughness exerts a noticeable effect on the timing of the hydrograph peak but has little impact on the volume or the magnitude of the peak. The peak was delayed approximately 5 minutes in the rough model, while the peak of the smooth model arrived 5 minutes earlier than the base case. The magnitude of the peak is slightly higher in the smoother case. For all three cases the initial soil moisture was 1.0 and the hydraulic conductivity of the channel was 27 mm/hr.

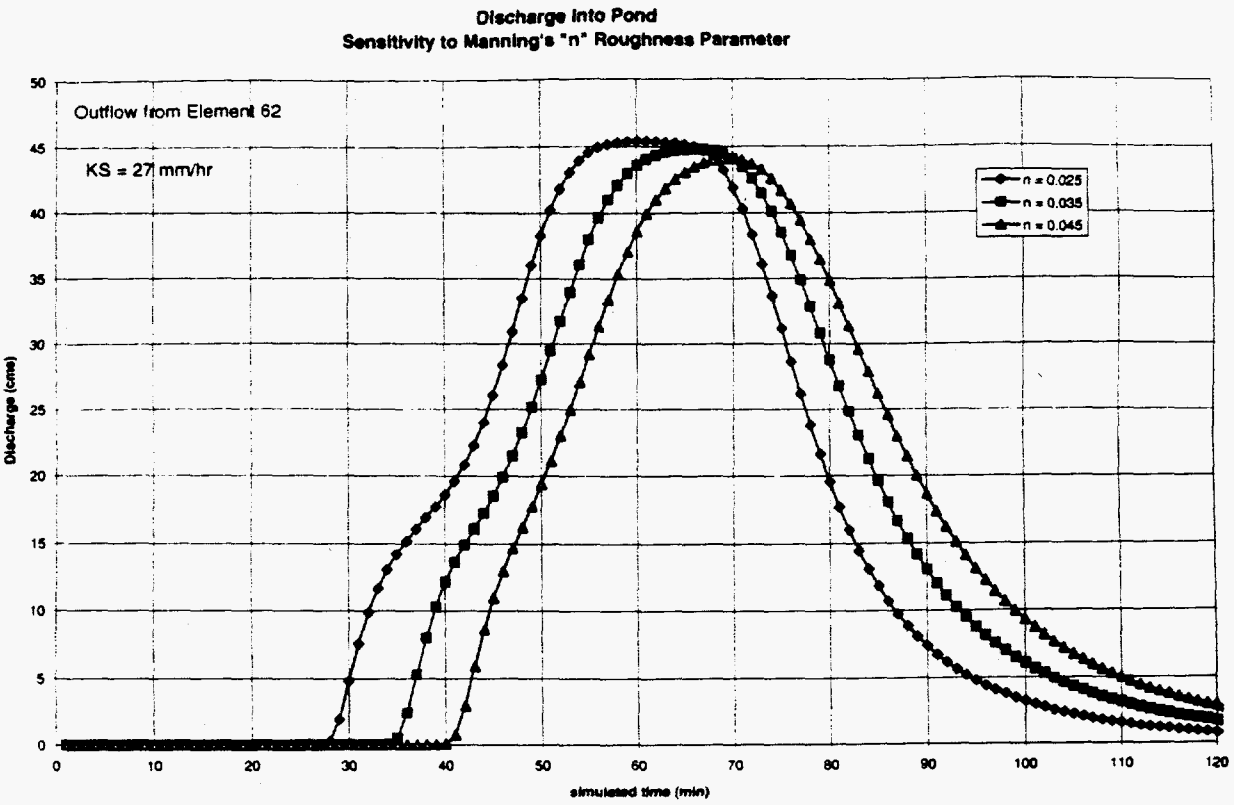

Figure 17

Sensitivity to Hydraulic Roughness, Manning's "n"

The timing of the hydrograph peak is shifted 5 minutes earlier or later in response to changes of Manning' n; however, the peak rate and volume are not significantly affected. (n=0.025 is smoother, n=0.045 is rougher)

This collection of sensitivity runs have identified the hydraulic conductivity of the channel and the initial soil moisture value as the most sensitive input parameters. Hydraulic roughness is less important. The Manning's value of 0.035 for the channel is considered suitable; however, the values for the plane elements on the mesa tops, walls, and canyon floor should be improved. The sensitivity to these values is not expected to be significant.

In addition to these three parameters, two other issues of sensitivity should be considered. They are the number of elements used to represent the watershed and the definition of the precipitation input. These two issues have been addressed in a number of papers in greater detail than I could do with the Big Buck Canyon model, thus I will summarize the findings of these papers rather than attempt an independent sensitivity study.

Goodrich (1994) presents the simulations results for the 631 hectare Walnut Gulch watershed in Arizona. This is similar in size to the Big Buck Watershed area which is 554 hectares. They differ in topography and land use (Walnut Gulch is rangeland while Big Buck Canyon is a steep narrow canyon); otherwise, the two sites are similar in terms of size and climate.

David Goodrich is one of the developers of the KINEROS program. He places a strong emphasis on the definition of the precipitation inputs and considers precipitation to be the most sensitive input to a simulation. This concern for the definition of precipitation is based simulations of the Walnut Gulch watershed and from other work with the program. Goodrich (1994) considered the difference between the used of 10 rain gauges and 1 gauge. He also demonstrates the effect of various numbers of model elements used to represent the same area. Figure 18 is a figure from Goodrich (1994) reproduced here to show the observed and simulated hydrographs for a runoff event on 1 August 1990. The figure shows four simulated hydrographs compared to the observed hydrograph. The four simulated hydrogaphs are reasonably similar to one another in spite of different numbers of rain gauges, model elements, or techniques of estimating the initial soil moisture. In the legend, the markers identified with "PBMR-256 Ele. SI input" represent a 256 element model with initial soil moisture determined from aircraft remote sensing (PBMR means push broom microwave radiometer). Notice that there is little difference between the simulation using 1 element and 256 elements. Unfortunately, all of the simulated hydrographs significantly over predict the hydrograph peak and volume. The timing of the peak and the shape of the simulated hydrographs are similar to the observed.

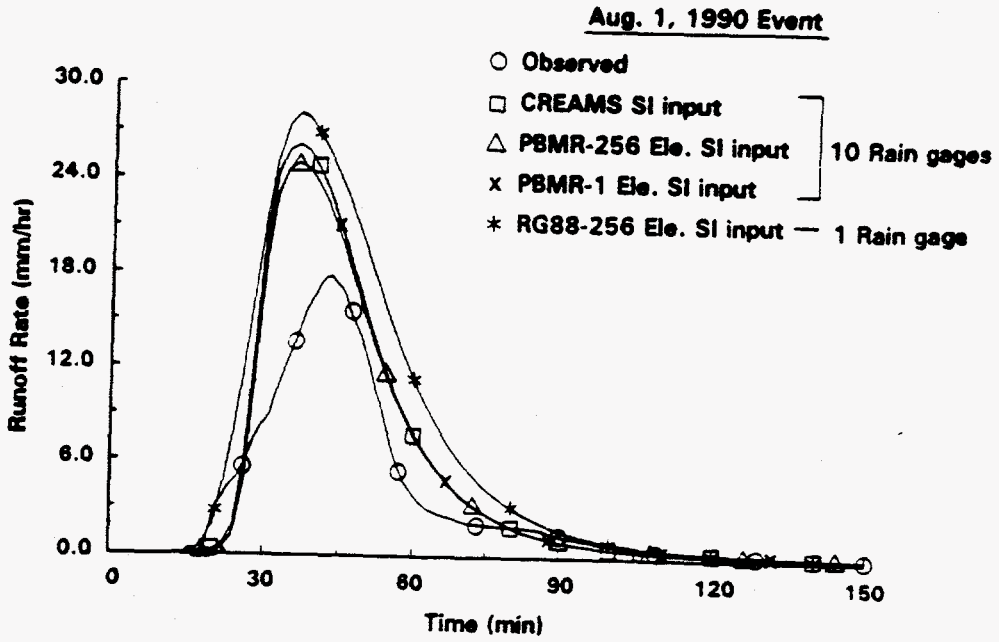

Figure 18

Sensitivity to the number of model elements

Simulated hydrographs overpredict flow compared with observed hydrograph at the Walnut Gulch watershed, Arizona. Negligible difference between the model with 256 elements and only one element. Source: Goodrich et. al. (1994) p. 1402, Figure 10

While sediment transport is not apart of the KINEMAT program, it is a part of the KINEROS program. The old version of KINEROS supported six different relations to determine the sediment transport capacity of the flow. These relations include the tractive force method, Yang's stream power method, the Bagnold/Kilinc method, the Ackers and White method, Yalin's method, and the Engelund/Hansen method. Appendix I presents the formulation of the erosion and sediment transport equations used in KINEROS. It also presents simulation results using a simple model that was run with all six transport capacity relationships. The highest sediment concentrations resulted from the used of the Bagnold method and the Acker and White method. These concentrations seemed unrealistically high. The lowest concentrations were produced with Yalin's method and the Engelund/Hansen method. Intermediate concentrations were predicted by Yang's method and by the tractive force method.

Additional information and guidance will be needed before a method can be selected for Big Buck canyon. When the release of the new KINEROS-II program is available, sediment transport can be added to the simulation model.

3.3.3 Future Modeling Work

Currently, the model of Big Buck canyon is operational and has been tested for sensitivities to input parameters, but it has not been calibrated. This section will outline model work that could be pursued in the future, such as calibration, sediment modeling, reconstruction of past flows, and flood frequency analysis.

The current model still need work to be calibrate qualitatively to the flood in 1991. Additional runoff events in August and September 1993 can also be used for calibration. The stream gauging data based on the pressure transducers is not meaningful in terms of stage, but the timing of the events could be used to check the simulation results. The precipitation data for these two events in 1993 is available for input to the program.

Another form of calibration is the simulation of major storms that have not produce runoff. Even a non-runoff event contains valuable information on the infiltration capacity of the watershed. For example, during my August 1994 trip to Los Alamos, there were some heavy rains on the day I arrived. I expected that such a large storm would have produced runoff, but it did not. A calibrated model should predict no flow in the channel when in fact there was no flow. If the simulation predicts flow when there was none, then information is gained on the calibration of the model. Thus, non-events are also opportunities to check the performance of the model.

Once the revised KINEROS-II program is released, the model will need further development to define the sediment characteristics and to choose a suitable sediment transport relation (such as Yalin's method or the Engelund/Hansen method). In the revised program, compound channel cross sections can be defined, two soil layers can be defined, and a distribution of sediment grainsizes can be defined. Calibration of the sediment

is a factor, then this two-phase flow phenomenon is not simulated by the model. Transmission losses continue to be an area of uncertainty that needs to be considered further.

The accounting of infiltration in the present KINEMAT program needs to be improved. For very high infiltration rates, the program output does not account for the inflow and outflow terms completely. The net simulation results appear reasonable, but the output summary values do not account for all the water on each element; thus, a large error residual value for some elements is produced. This may be a bug in the output or it may be a bug in the simulation of infiltration. The new KINEROS-II results will need to be checked to see if this bug has been resolved.

Overall, I am pleased with the capabilities of KINEROS. The program is well suited to the watershed scale of Big Buck Canyon and the need for high spatial variability of soil properties and precipitation inputs. The complexity of the program seems to be well balanced between the need to represent detailed physical processes while not being awkward to understand or to construct the input files. The new KINEROS-II should be a positive step forward in modeling the hydrologic response of the watershed. I recommend that future modeling work continue with the new program.

4. Water Chemistry

The water chemistry experiments performed by Russ Herrin measured the amount of various metals associated with the channel sediments and the amount of the metals that can be leached from the sediment by water. These laboratory experimental results need to be integrated with the simulated sediment transport results to estimate the movement of contaminants through the watershed. The formal linkages between the chemistry results and the water/sediment modeling results have not yet been defined. An enrichment ratio approach (Lane 1985) is the most likely route.

4.1 Leaching and Digestion Experiments by Russ Herrin

There are two mechanisms for transporting contaminants during a runoff event. First, contaminants associated with the sediment (either adsorbed to surfaces or mixed into the bulk volume) are moved when the sediment itself is eroded and transported by the flow. Second, contaminants can dissolved into the water and be carried through the watershed as far as the flow is sustained. Thus, the solid and dissolved phases need to be considered. Herrin (1994) measured the concentration of contaminants in the solid phase associated with the sediment by digesting soil samples and analyzing them with atomic emission spectroscopy (ICP-AES). Additional soil samples were mixed with pH adjusted water to leach contaminants from the soil mixture. The dissolved phase concentrations were then measured using a mass spectrometer (ICP-MS).

Samples were tested for six metals: barium, beryllium, cadmium, lead, nickel, and uranium. Concentrations of all metal were low and sometimes below the detection limit. The results for barium were the most accurate. Barium concentrations in the solid phase ranged from 58 to 460 μg/g; well above the detection limit of 4.1 μg/g. When exposed to water in the leaching experiments, approximately 4% of the solid barium was converted into the dissolved phase.

calibrated, the model can be used to generate a synthetic record of flow for flood frequency analysis.

5.3 Water Chemistry

The experimental chemistry work of Herrin (1994) applies to Potrillo Canyon. Sediment samples collected from the channel at two locations were analyzed to determine the concentration of six heavy metals mixed with the sediment. The samples were also tested to determine the amount of each metal leach from the sediment into the dissolved phase when mixed with water. The six metal were uranium, nickel, barium, beryllium, cadmium, and lead. While these results may demonstrate the fraction of each material that can be leached into the dissolved phase, the total concentration of each metal may not be representative of the level of contamination in Big Buck Canyon.

The linkages between the chemistry results and the hydrologic results remains to be defined. This linkage is necessary before the movement of contaminants can be evaluated.

5.4 Recommendations

The following list of recommendations contains specific ideas that should be considered for the future progress of the research.

1. The rain gauge measurement interval should be reduce to 5 minutes. The current interval of 15 minutes was based on the sampling methods of the LANL weather stations. However, in the KINEMAT model, a shorter interval is easily accommodated and would improve the definition of the precipitation input to the model. Since common storm events are short (often less than one hour) a 5 minute data interval would improve the simulation results.

2. Obtain the new KINEROS-II program when it is released and update the input files for Big Buck Canyon to model the compound channel shape, to define two soil layers, and to define the distribution of sediment grainsizes to model sediment transport.

3. Study the phenomenon of transmission losses and determine how to define the effective hydraulic conductivity. The current method of measuring the hydraulic conductivity with the Guelph permeameter does not produce suitable input values for the model.

4. Compare the simulation results from the KINEROS program with those from the HSPF program.

5. Install a scour depth measurement sensors at the streamflow monitoring sites. The first choice would be a sonar traducer mounted to the bottom of the paddlewheel float. A low cost alternative would be the free falling probe that is attached to a potentiometer that will track the progression of downward scour but not the subsequent aggradation of sediment.

6. Install a total sediment load catch basket at the drop-off on the downstream end of the culvert under State Road 4. This would be a direct measure of the total sediment yield of the watershed.

Boers, Th. M. (1994). "Rainwater Harvesting in Arid and Semi-Arid Zones," ILRI Publication 55, International Institute for Land Reclamation and Improvement (ILRI), P.O. Box 45, 6700 AA Wageningen, The Netherlands

Bowles, Joseph E. (1992). *Engineering Properties of Soils and Their Measurement*, Fourth Ed., McGraw-Hill, Inc.

Breuser, H.N.C., and A.J. Raudkivi (1991). *Scouring, IAHR* 2, *Hydraulic Structures Design Manual* A.A. Balkema Publ., Brookfield, VT

Burkham, D.E. (1970). "A Method for Relating Infiltration Rates to Streamflow Rates in Perched Streams," USGS Professional Paper 700-D, p. D266-D271

Dietrich, W.E., T. Dunne, N.F. Humphrey, and L.M. Reid (1982). "Construction of Sediment Budgets for Drainage Basins", a contribution to *Sediment Budgets and Routing in ForestedDrainage Basins*, edited by F.J. Swanson, USDA Forest Service General Technical Report PNW-141, August 1982

Donigian, A.S. and W.C. Huber (1991). *Modeling of Nonpoint Source Water Quality in Urban and Non-urban Areas,* US EPA, Environmental Research Laboratory, Athens, GA EPA/600/3-91/039, June 1991

Dunn, Thomas, and Luna B. Leopold (1978). *Water in Environmental Planning* W.H. Freeman and Co. Publ., New York

Eagleson, Peter (1970). *Dynamic Hydrology,* McGraw-Hill, Inc.

Freeze, Allan, and John Cherry (1979). *Groundwater,* Prentice-Hall Publ.

French, Richard, editor (1990). *Hydrology and Hydraulics of Arid Lands*, ASCE Proceedings of Int'l Conference, San Diego, CA July 1990

Fullerton, W.T. (1983). "Water and Sediment Routing from Complex Watersheds" M.S. Thesis, Colorado State University, Fort Collins, CO (MULTSED model)

Gallaher, Bruce (1993). "Hydraulic Property Data for Bandelier Tuff," one page of informal information compiled by Bruce Gallaher, EM-8, LANL, 11 August 1993 A one page sheet of values of hydraulic conductivity and other values for Tshirege member, Tsankawi Pumice/Cerro Toledo member, and Otowi member tuff found on the mesa tops of Los Alamos.

Glysson, G. Douglas (1989). "Criteria for a Sediment Data Set," ASCE Sediment Transport Modeling Symposium 1989

Laronne, Johnathan B., Ian Reid, Yitshak Yitshak, and Lynne E. Frostick (1994). "The Non-Layering of Gravel Streambeds Under Ephemeral Flood Regimes," Journal of Hydrology Vol. 159, p. 353-363

Laronne, Johnathan B., and Ian Reid (1993). "Very High Rates of Bedload Sediment Transport by Ephemeral Desert Rivers," Nature, Vol. 366, 11 November 1993, p. 148

Leavesly, G.H., R.W. Lichty, B.M. Troutman, and L.G. Saindor (1983). *Precipitation-Runoff Modeling System: User's Manual,* USGS Water-Resources Investigations Report 83-4238, 207 pp. (PRMS model)

Leopold, Luna B., and John P. Miller (1956). "Ephemeral Streams - Hydraulic Factors and Their Relation to the Drainage Net," USGS Professional Paper 282-A

Leopold, Luna, M.G. Wolman, and John Miller (1964). *Fluvial Processes in Geomorphology,* W.H.Feeman and Co.

Linsley, Kohler and Paulhus (1982). *Hydrology for Engineers, 3rd Ed.* McGraw Hill Publ.

Michaud J. and S. Sorooshian (1994). "Comparison of Simple verses Complex Distributed Runoff Models on a Midsized Semiarid Watershed," *Water Resources Research,* Vol. 30, No. 3, p. 593, March 1994

Maidment, D.R. editor (1993). *Handbook of Hydrology,* McGraw Hill Publ., Chapter 21: Computer Models for Surface Water, by Johannes DeVires and T.V Hormadka

Meselhe, E.A. and F.M. Holly Jr. (1993). "Simulation of Unsteady flow in Irrigation Canals with Dry Bed," ASCE *Journal of Hydraulic Engineering,* Vol. 119, No. 9, p. 1021, Sept. 1993

Rao, Achanta Ramakrishna, Vedula Subrahmanyam, S. Thayumanavan, and Damodaran Namboodiripad (1994). "Seepage effects on sand-bed channels," ASCE *Journal of Irrigation and Drainage* Vol. 120, No. 1, Jan/Feb 1994, pp. 60-79

National Research Council (1991) *Opportunities in the Hydrological Sciences*

Nyhan, J.W, L.W. Hacker, T.E. Calhoun, and D.L. Young (1978). "Soil Survey of Los Alamos County, New Mexico," Los Alamos Scientific Laboratory, Informal Report LA-6779-MS, UC-11, June 1978

Smith, Chery, Renard, and Gwin (1982). "Supercritical Flow Flumes for Measuring Sediment-Laden Flow," USDA ARS Technical Bulletin 1655, July 1982

Singer, Michael and Donald MUNNS (1991). *Soils, an introduction,* Macmillan Publishers

Sorman, A.U., and M.J. Abdulrazzak (1993). "Flood Hydrograph Estimation for Ungaged Wadis in Saudi Arabia," ASCE Journal of Water Resources Planning and Management, Vol. 119, No. 1 Jan/Feb. 1993, p. 45

USDA-SCS (1985). *National Engineering Handbook-Section 4: Hydrology*

USGS (1977). *National Handbook of Recommended Methods for Water-Data Acquisition*

Walters, Michael O. (1990). "Transmission Losses in Arid Region," *Journal of Hydraulic Engineering,* Vol. 116, No. 1, January 1990, ASCE

Walters, Michael O. (1989). "A unique flood event in an arid zone," *Hydrological Processes,* Vol. 3, pp. 15-24

World Meteorological Organization (1994). *Guide to Hydological Practices,* Fifth Edition, WHO-No. 168

World Meteorological Organization, 19--. *Hydrology Operational Multipurpose System (HOMS) Reference Manual (HRM),* Section K: Hydrological analysis for the planning and design of engineering structures and water-resource systems.
Available from the HOMS National Reference Center in the United States, contact Eugene A. Stallings, Director, HOMS NRC for the United States, NOAA, National Weather Service, Office of Hydrology, W/OH22, 1325 East-West Highway, Rm 8140, Silver Springs, MD 20910-3283

Woolhiser, D.A., R.E. Smith, D.C. Goodrich (1990). "KINEROS, A Kinematic Runoff and Erosion Model: Documentation and User Manual," USDA, Agricultural Research Service, Tuscon AZ, publication no. ARS-77

Water Resorces Research , Vol. 30, No. 5, May 1994: Special Section: Monsoon 90

Zevenbergen, L.W. and M.R. Peterson (1988). "Evaluation and Testing of Storm-Event Hydrologic Models," ASCE Proceedings of the National Conference on Hydraulic Engineering, Colorado Springs, CO, August 1988, p. 467